DAFTAR PUSTAKA

Abdelnaeim, M.Y., El Sherif, I.Y., Attia, A.A., and 2016. Impact Of Chemical Activation On The Adsorption Performance Of Common Reed Faraji Towards Cu (II) and Cd (II). *Int J Miner Process*. 157, 80–88.

Abioye, A.M., and Ani, F.N., 2015. Recent Development In The Production Of Activated Carbon Electrodes From Agricultural Waste Biomass For Supercapacitors. *Renewable and Sustainable Energy Reviews*. 52, 1282–1293.

Abulizi, A., Yang, G.H., Okitsu, K., and Zhu, J., 2014. Synthesis Og MnO_2 Nanoparticle From Sonochemical Reduction Of MnO In Water Under Different pH Condutions. *Ultrasonics sonochemistry*. 21, 1629-1634.

Akbari, S., Foroughi, M.M., and Ranjbar, M., 2018. Solvent-free Synthesis and Characterization of MnO_2 Nanostructures and Investigation of Optical Properties. *J Nanomed Nanotechnol*. 3, 1-9.

Ali, A., Shah, T., Ullah, R., Zhou, P., Guo, M., Ovais, M., Tn, Z., and Rui, Y., 2021. Review On Recent Progress In Magnetic Nanoparticle; Synthesis, Chaarakterization and Diverse Aplictions. *Frontiers In Chemistry*. 9, 1-25.

Allcott, H., and Wozny, N., 2014. Gasoline Prices, Fuel Economy, and the Energy Paradox*. The Review of Economics and Statistics*. 5, 779-795.

Alsadi, J.K. and Esfandiari, N., 2019, Synthesis of Activated Carbon from Sugarcane Bagasse and Application for Mercury Adsorption, *Pollution*, 5, 585-596.

Anca-Couce, A., 2016. Reaction Mechanisms And Multi-Scale Modelling Of Lignocellulosic Biomass Pyrolysis. *Progress in Energy and Combustion Science*. 53, 41 – 79.

Antonucci, P. L., and Antonucci, V., 2011. *Electrochemical Energy Strorage*, In Tech China. Shanghai.

Arazi, I., and Putra, A., 2020. Preparation and Characterization Composites Of Activated Carbon From Cassava Peel (Manihot Utillisima)-Copper (II) Oxide (CuO) As A Thermoelectric Material. *International Journal Of Research and Review*. 9, 2454-2237.

Augustyn, V., Simon, P., and Dunn, B., 2014. Pseudocapacitive oxide materials for high-rate electrochemical energy storage*,* Open Archive Toulouse Archive Ouverte. *Energy & Environmental Science*. 7, 1597-1614.

Balakrishnan, A., and Subramanian, K. R.V., 2014. *Nanostructured Ceramic Oxides For Supercapacitor Application*, CRC Press Taylor & Francis Group Landon New York.

Bapa, Y., and Botahala. L., 2019. Effect Of The Contact Time Of Candlenut Shell Charcoal and H_3PO_4 Activator As On The Purification Process Of Used Cooking Oil Indonesia. *Chimica Acta*. 2, 104-110.

Baseri, J.R., Palanisamy, P.N., and Sivakumar, P., 2012. Preparation and Characterization Of Activated Carbon From Thevetia Peruviana For The Removal Of Dyes From Textile Waste Water. *Advances In Applied Science Research*. 3, 377-383.

Bhujun, B., Tan, M.T.T., and Shanmugam, A.S., 2017. Study Of Mixed Ternary Transition Metal Ferrites As Potential Electrodes For Supercapacitor Applications. *Results In Physics*. 7, 345-353.

Burke, A., 2007. Considerations For The Performance And Application Of Electrochemical Capacitors*. Electrochimica Acta.* 53, 1083-1091.

Butterfielda, C.N., Soldatovab, A.V., Leea, S., Spirob, T.G., and Tebo, B.M., 2013. Mn (II,III) Oxidation and MnO_2 Mineralization By An Expressed Bacterial Multicopper Oxidase. *PNAS*.110, 11731–11735.

Cao, J. Pan, Y., Jiang, Y., Qi, R., Yuan, B., Jia, Z., Jiaang, J., and Wang, Q., 2020. Computer-Aired Nanotoxicology: Risk Assessment Of Metal Oxide Nanoparticles Via Nano-QSAR. *Green Chemistry.* 22, 3512-3521.

Cao, Z., Yang,Y., Qin, J., and Su, Z., 2021. A core-shell porous MnO_2/Carbon Nanosphere Composite As the Anode Of Lithium-Ion Batteries. *Journal of Power Sources.* 491, 1-9.

Chang, J.K., Huang, C.H., Lee, M.T., Tsai, W.T., Deng, M.J., and Sun, I.W., 2009. Physicochemical Factors That Effct The Pseudocapacitance And Cyclic Stability Of Mn Oxide Electrodes. *Electrochim. Acta*. 54, 3278–3284.

Chao, X., Zhong, L., Peng, X., Sun, S., Li, S., Liu, S., and Sun, R., 2014. Comparative Study Of The Pryrolisis Of Ligonecellulose And It Major Componetnts,: Characterization And Overall Distribution Of Their Biochars And Volatile Bioreseource*. Technology.* 155, 21-27.

Chen, A., and Holt-Hindle, P., 2010. Platinum-Based Nanostructured Materials: Synthesis, Properties, and Applications, *Chem. Rev*. 110, 3767–3804.

Chen, Q. Chen, J. Zhou, Y. Song, C. Tian, Q. Xu, J. Wong, C.P., 2018, Enhancing Pseudocapacitive Kinetics Of Nanostructured MnO_2 Through Anchoring Onto Biomassderived Porous Carbon*. Applied Surface Science.* 440, 1027–1036.

Chen, W., Rakhi, R. B., Hu, L., Xie, X., Cui, Y., and Alshareef, H. N., 2011. High-Performance Nanostructured Supercapacitors on a Sponge. *Nano Lett*. 11, 5165–5172.

Chen, W., Fan, Z., Gu, L., Bao, X., and Wang, C., 2010. Enhanced Capacitance Of Manganese Oxide Via Confinement Inside Carbon Nanotube. *Chemical Communications.* 46, 3905-3907.

Chen, X., Paul, R., and Dai, L., 2017. Carbon-Based Supercapaciors For Efficient Energy Stronge. *National Science Review.* 4, 453-489.

Chen, Z., Zheng, L., Zhu, T., Ma, Z., Yang, Y., Wei, C., Liu, L., and Gong, X., 2019. All-Solid-State Flexible Asymmetric Supercapacitors Fabricated By The Binder-Free Hydrophilic Carbon Cloth@MnO_2 and Hydrophilic

Carbon Cloth@Polypyrrole Electrodes. *Advanced Science News*. 1, 1-9.

Chen, Q., Zhang, T.C., Ouyang, L., and Yuan, S., 2022. Single-Step Hydrothermal Synthesis of Biochar from H_3PO_4-Activated Lettuce Waste for Efficient Adsorption of Cd(II) in Aqueous Solution. *Molecules*. 27, 1-20.

Cho, M.H., Choi,E.S., Kim, S., Goh, S.H., and Choi, Y., 2017. Redox-Responsive Manganese Dioxide Nanoparticles For Enhanced MR Imaging And Radiotherapy Of Lung Cancer. *Frointiers In Chemistry*. 5, 1-10.

Cho, Y.S., Kim, H., Byeon, M., Kim, D.B., Park, H., Jung, Y., Bae, Y., Kim, M., Lee, D.J., Park, J.O., Kang, K.I,D., and Park, C.R., 2020. Enhancing the Cycle Stability of Li-O_2 Batteries via Functionalized Carbon Nanotubebased Electrodes. *J. Mater. Chem. A*,8, 4263-4273.

Choi, H.S., and Park, C.R., 2014. Theoretical Guidelines To Designing High Performance Energy Storage Device Based On Hybridization Of Lithium-Ion Battery And Supercapacitor. *Journal of Power Sources. 259.* 1–14.

Choi, J.R., Lee, J., Yang, G., Heo, Y.J., and Park, S.J., 2020. Activated Carbon/MnO_2 Composites as Electrode for High Performance Supercapacitors. *Catalysts.* 256, 1-10.

Cremonessi, J.M.D.O., Tiba, D.Y., and Domingues. S.H., 2020. Fast Synthesis of δ -MnO_2 For High-Performance Supercapcitor Electrode. *SN Apllied Science*. 2, 1-9.

Darmawan, S., Wistara, N.J., Pari, G., Maddu, A., and Syafii, W., 2016. Characterization of Lignocellulosic Biomass as Raw Material for the Production of Porous Carbon-based Materials. *BioResources*. 11, 3561- 3574.

Dawoud, H.D., Al Tahtamouni, T., and Bensalah, N., 2019. Sputtered Manganese Oxide Thin Film On Carbon Nanotubes Sheet As A Flexible And Binder-Free Electrode For Supercapacitors. *International Journal Of Energy Research*. 43, 1245-1254.

Demiral, I., and Samdan C.A., 2016. Preparation and Characterisation Of Activated Carbon From Pumpkin Seed Shell Using H_3PO_4. *Anadolu University Journal of Science and Technology A-Applied Sciences and Engineering.* 17, 125–13.

Deng, D., Kim, B.S., Gopiraman, M., and Kim, I.S., 2015. Needle-Like MnO_2/Activated Carbon Nanocomposites Derived From Human Hair As Versatile Electrode Materials For Supercapacitors. Royal Society of Chemistry. 5, 81492–81498.

Dessiea, Y., Tadesse, S., and Eswaramoorthy, R., 2020. Physicochemical Parameter Influences And Their Optimization On The Biosynthesis Of MnO_2 Nanoparticles Using Vernonia Amygdalina Leaf Extract. *Journal Pre-Proofs*. 1,1-35.

Deyuso, A.M., Rubio, B., and Izquierdo, M.T., 2014. Infuence Of Activation Atmosphere Used In The Chemical Activation Of Almond Shell On The Characteristics And Adsorption Performance Of Activated Carbons. *Fuel Process Technology*. 119, 74–80.

Dhahri, R., Yılmaz, M., Mechi, L., Alsukaibi, A.K.D., Alimi, F., Salem, R.B., and Moussaoui, Y., 2022. Optimization of the Preparation of Activated Carbon from Prickly Pear Seed Cake for the Removal of Lead and Cadmium Ions from Aqueous Solution. *Sustainability*. 14, 1-17.

Ding N., Prsasd, K., and Lie T.T. 2017. The Electric Vehicle. *Int. J. Electric and Hybrid Vehicles.* 1,49-66.

Diharyo., Salampak., Damanik, Z., dan Gumiri, S., 2020. Pengaruh Lama Aktifasi Dengan H_3Po_4 Dan Ukuran Butir Arang Cangkang Kelapa Sawit Terhadap Ukuran Pori Dan Luas Permukaan Butir Arang Aktif. *Prosiding Seminar Nasional Lingkungan Lahan Basah*. 5, 48-54.

Doloksaribu, M., Harsojo., Triyana, K., and Prihandoko, B., 2017. The Effect Of Concentration Nanoparticles MnO_2 Doped In Activated Carbon As Supercapacitor Electrodes. *Applied Engineering*. 19, 8625-8631.

Dong, D., Zhang, Y., Xiao, Y., Wang, T., Wang, J., Romero, C.E, and Pan, W.P., 2020. High Performance Aqueous Supercapacitor Based On Nitrogen-Doped Coal-Based Activated Carbon Electrode Materials. *J Colloid Interface Sci*. 580, 77–87.

Du, J.S., Sun, B., Zhang, J., and Guan, X. H., 2012. Parabola-Like Shaped pH-Rate Profile For Phenols Oxidation by Aqueous Permanganate. *Environmental Science & Technology.* 46, 8860-8867.

Ekpete, O.A., Marcus, A.C., and Osi, V., 2017. Preparation and Characterization of Activated Carbon Obtained from Plantain (Musa paradisiaca) Fruit Stem. *Journal of Chemistry.* 1,1-7.

Feng, X.H., Wang, P., Shi, Z.Q., Kwon, K.D., Zhao, H.Y., Yin, H., Lin, Z., A, M. Q., Liang, X.R., Liu, F., and Sparks, D. L., 2018. A Quantitative Model For The Coupled Kinetics Of Arsenic Adsorption/Desorption And Oxidation On Manganese Oxides. *Environmental Science & Technology Letters.* 5, 175-180.

Frackowiak, E., 2007. Carbon Materials For Supercapacitor Application. *Physical Chemistry Chemical Physics.*15, 1774–1785.

Gawande, P.R., and Kaware, J., 2017. Characterization And Activation Of Coconut Shell Activated Carbon. *International Journal Of Engineering Science Invention.* 11, 43-49.

Gehrke, V., Maron, G.K., Rodrigues, L.D.S., Alano, J.H., Pereira, C.M.P.D., Orlandi, M.O., and Carreno, N.L.H., 2020. Facile Preparation of a Novel Biomass-Derived H_3PO_4 And $Mn(NO_3)_2$ Activated Carbon From Citrus Bergamia Peels For High-Performance Supercapacitors. *Materials Today Communications.* 26, 1-32.

George, J.M., Antony, A., and Mathew, B., 2018. Metal oxide Nanoparticles In Electrochemical Sensing and Biosensing: A review. *Microchimica Acta*. 185.

Goertzen, S. L., Theriault, K. D., Oikcle, A. M., Tarasuk, A. C., and Andreas, H. A., 2010. Standardization of The Boehm titration. Part I. CO_2 Expulsion and Endpoint Determination. *Carbon*. 48,1252 – 1261.

Grote, F., Kuhnel, R.S., Balducci, A., and Lei, Y., 2014. Template Assisted Fabrication Of Free-Standing MnO_2 Nanotube and Nanowire Arrays And Their Application In Supercapacitors. *Applied Physics Letters*. 104, 1-4.

Guo, C.H., Sun, T., Cao, F., Liu, Q., and Ren, Z., 2014. Metallic Nanostructures For Light Trapping In Energy-Harversting Devices. *Science & Applications*. 3, 1-12.

Halimah, S.N., 2016. *Pembuatan dan Karakterisasi Serta Uji Adsorpsi Karbon Aktif Tempurung Kemiri (Aleurites Molucana) Terhadap Metilen Biru*. Skripsi Tidak Diterbitkan, Fakultas Matematika Dan Ilmu Pengetahuan Alam Universitas Lampung. Bandar Lampung.

Halper, J.C.E., and Halper M.S., 2006. Supercapacitors: A Brief Overview. *Mitre Nanosystems Group*.

Hammad, E.N., Hammad, Salem, S.S., Mohamed, A.A., and El-Dougdoug, W., 2022. Environmental Impacts of Ecofriendly Iron Oxide Nanoparticles on Dyes Removal and Antibacterial Activity. *Applied Biochemistry and Biotechnology*. 1-15.

Han, X., Zhang, F., Wan, J., Xu, W., Li J., Hu, C., Liu, G., and Cheng, X., 2020. An Activated Carbon Cloth Anode Obtained With a Fast Molten Salt Method for High-performance Supercapacitors. *Journal of Alloys and Compounds*. 3, 1-9.

Hannan, M., Hoque, M., Mohamed, A., and Ayob, A., 2017. Review Of Energy Storage Systems For Electric Vehicle Applications: Issues And Challenges. *Renewable and Sustainable Energy Reviews.* 69, 771–789.

Himmaty, I., dan Endarko, 2013. Pembuatan Elektroda dan Perancangan Sistem Capacitive Deionization untuk Mengurangi Kadar Garam pada Larutan Sodium Clorida (NaCl). *Berkala Fisika*. 3, 67–74.

Ho, C.H., Triolo, J.H., Elias, A.L., Kilgore, K.L., Dimarco, A.F., Bogie, K., Vette, A.H., Audu, M.L., Kobetic, R., Chang, S.R., Chan, K.M., Dukelow, S.M.D, Bourbeau, J.M., Brose, S.W., Gustafson, K.J., Kiss, Z.H.T., and Mushahwar, V.K., 2014. Functional Electrical Stimulation and Spinal Cord Injury, *Physical Medicine and Rehabilitation Clinics Of North American.* 25, 631–654.

Hu, Z., Xiao, X., Chen, C., Li, T., Huang, L., Zhang, C., Su, J., Miao, L., Jiang, J., Zhang, Y., and Zhou, J., 2015, Al-doped α-MnO_2 For High Mass-Loading Pseudo-Capacitor With Cycling Stability. *Nano Energy*. 11, 226-234.

Huang, X., Lv, D., Zhang, Q., Chang, H., Gan, J., and Yang, Y., 2010. Crystalline Macroporous $BMnO_2$: Hydrothermal Synthesis and Application In Lithium Battery. *Electrochimica Acta*. 55, 4915–4920.

Huang, Y., Zheng, M., Lin, Z., Zhao, B., Zhang, S., Yang, J., Zhu, C., Zhang, H., Sun, D., and Shi, Y., 2015. Flexible Cathodes A Multifunctional Interlayers Based On Carbonized Bacterial Cellulose For High-Performance Lithium–Sulfur Batteries. *Journal of Materials Chemistry A*. 3, 10910–10918.

Huang, Z.H., Song, Y., Feng, D.Y., Sun, Z., Sun, X., and Liu, X.X., 2018. High Mass Loading MnO_2 With Hierarchical Nanostructures For Supercapacitor*s. American Chemical Society*. 12, 3557–3567.

Igwegbe, C.A., Umembamalu, C.J., Osuagwu, C.U., Oba, S.N., and Emembolu, L.N., 2021. Studies on Adsorption Characteristics of Corn Cobs Activated Carbon for the Removal of Oil and Grease from Oil Refinery Desalter Effluent in a Downflow Fixed Bed Adsorption Equipment. *European Journal of Sustainable Development*. 1,1-14.

Iro, Z.S., Subramani, C., and Dash, S.S., 2016. A Brief Review On Electrode Materials For Supercapacitor. *International Journal of Electrochemical Science.* 11, 10628 – 10643.

Iwanow, M., Gartner, T., Sieber, V., and Konig, B., 2020. Activated Carbon As Catalyst Support:Precursors, Preparation Modification and Characterization*. Beilstein Journal of Organic Chemistry.* 16, 1188–1202.

Jaganyi, D., Altaf, M., and Wekasa, I., 2013. Synthesis and Characterization of Whisker-Shaped MnO_2 Nanaostructure at Room Temperature, *Applied Nanoscience.* 3, 329-333.

Jayalakshmi, M., and Balasubramanian, K., 2008. Simple Capacitors To Supercapacitors-An Overview. *International Journal of Electrochemical Science.* 11, 1196-1217.

Ji, Q., Li, H., and Zhang, J., 2020. Preparation And Characterization of Bio-Based Activated Carbon From Fish Scales. *Bioresources*. 16, 614-621.

Jiang, J., 2011. Use Of Manganese Compounds And Microbial Fuel Cells In Wastewater Treatment, KTH Land and Water Resources Engineering, 16, 1-43.

Jing, W., Yan, Y., Kim, I., and Sarvi, M., 2016. Electric Vehicles: A Review Of Network Modelling And Future Research Needs. *Advances In Mechanical Enginering*. 1, 1–8

John, R.I., and Hem, D., 1963. *Chemical Equilibria and Rates of Manganese 'Oxidation, Nited States Government Printing Office*. Washington.

Jovanovic, I.R., Colleen M. B.C., Ramsey. B., Wayne W.L., Benjamin P.B., Donna M., and Lynn C.F., 2020. Strategies for the Photoreduction of Tc-99 Pertechnetate to Low-Valent Tc by Keggin Polyoxometalates. *European Journal of Inorganic Chemistry. 22,1-2*.

Jyothibasu, J.P., Wang, R.H., Ong, K.O., and Juping H.I., 2021. Cellulose/Carbon Nanotube/MnO_2 Composite Electrodes With High Mass Loadings For Symmetric Supercapacitors. *Cellulose.* 28, 3549-3567.

Kasim, A.H., Zakir, H., Raman, M., and Abdussamad, B., 2017. Redox Deposition Of MnO_2 Nanoparticles On Rice Husk Based Activated Carbon As High-Performance Electrode Material For Pseudo-Capacitors . *Indonesia Chimica Acta. 1, 44-58.*

Kaushik, M., and Moores, A., 2016. Nanocelluloses As Versatile Supports For Metal Nanoparticles And Their Applications In Catalysis. *Royal Society Of Chemistry.* 18, 622-637.

Kazazi, M., 2018. Effect Of Electrodeposition Current Density On The Morphological and Pseudocapacitance Characteristics Of Porous Nano-Spherical MnO_2 Electrode. *Ceramics International*. 44, 10863-10870.

Kiamahalleh, M.V., Zein, S.H.S., Najafpour, G., Sata, S. A., and Buniran, S., 2012. Multiwalled Carbon Nanotubes Based Nanocomposites For Supercapacitors: *A Review Of Electrode Materials. Nano* . 7.

Kim, B.K., Sy, S., Yu, A., and Zhang., 2015. Electrochemical Supercapacitors For Energy Stoge Add Conversion, Handbook Of Clean Energymsystem.

Kim, H., Watthanphanit, A., and Saito, N., 2016. Synthesis of Colloidal MnO_2 With a Sheet-Like Structure By One-Pot Plasma Discharge In Permanganate Aqueus Solution. *Royal Society of Chemistry.* 6, 2826-2834.

Kong, S., Jin, B , Quan, X., Zhang, G., Guo, X., Zhu,X., Yang, F., Cheng, K., Wang, G., and Cao, D., 2019. MnO_2 Nanosheets Decorated Porous Active Carbon Derived From Wheat Bran For High-Performance Asymmetric Supercapacitor. *Journal Of Electroanalytical Chemistry*. 850, 1-8.

Kouchachvili, L., Yaici, W. and Entchev, E., 2018. Hybrid Battery/supercapacitor Energy Storage System for the Electric Vehicles. *Journal Power Sources*. 374, 237–248.

Krisnawati, H., Kalio, M., and Kanninen M., 2011. *Aleurites Moluccana (L) Wild*, Center For International Forestry Research. Bogor.

Kristianto, H., 2017, Review: Sintesis Karbon Aktif Dengan Menggunakan Aktivasi Kimia $ZnCl_2$. *Jurnal Integrasi Proses*. 6,105.

Kumar D, Kumar G, Das R, and Agrawal V., 2018. Strong Larvicidal Potential Of Silver Nanoparticles (Agnps) Synthesized Using Hol-Arrhena Antidysenterica (L.) Wall. Bark Extract Against Malarial Vector Anopheles Stephensi. *Liston Process Saf Environ*. 116,137– 148.

Kumar, Y., Chopra, S., Gupta, A., Kumar, Y., Uke, S.J., and Mardikar, S. P., 2020. Low Temperature Synthesis Of MnO_2 Nanostructures For Supercapacitor Application. *Materials Science For Energy Technologie*. 1, 1-26.

Lan, S., Wang, X.M., Yang, P., Qin, Z.J., Zhu, M.Q., Zhang, J., Liu, F., Tan, W.F., Huang, Q. Y., and Feng, X.H., 2019. The Catalytic Effect Of Aqds As An Electron Shuttle On Mn(II) Oxidation To Birnessite On

Ferrihydrite At Circumneutral pH. *Geochimica et Cosmochimica Acta*. 247, 175-190.

Laos, L. E. Aji, M.P., dan Suhaldi., 2016*. Pengaruh Konsentrasi Karbon Aktif Kemiri Dan Aplikasinya Terhadap Penjernihan Limbah Cair Methylene Blue*. 5, 141-144.

Latupeirissa, J., Tanasale, M.F.J.D.P., and Dade, K., 2017. Carbon Characterization From Candlenut Shells (Aleurites Moluccana (L) Wild) With X-RD. *Indonesian Journal of Chemical Research.* 3, 326 – 330.

Lee, H.N., An, K., P, S.J. S, and Kim, B., 2019. Mesopore-Rich Activated Carbons For Electrical Double-Layer Capacitors by Optimal Activation Condition. *Nanomaterial*. 4,1-9.

Lempang, M., Syafii, W., dan Pari, G., 2011.Struktur dan Komponen Arang Serta Arang Tempurung Kemiri. *Jurnal Penelitian Hasil Hutan*. 23, 278-294.

Li, K., Han, K., and Li, S., 2018. Porous Carbons From Sargassum Muticum Prepared by H_3PO_4 and KOH Activation For Supercapacitors. *Journal of Materials Science*. 1, 1-13.

Li, X.S., Xu, M.M., Yang, Y., Huang, Q.B., Wang, X.Y., Ren, J.L., and Wang, X.H., 2019. MnO_2 @Corncob Carvon Composite Electrode and All- Solid-Slate Supwercapacitor With Improved Electrochemical Ferformance. *Material.* 2379, 1-12.

Liu, j., Song, X., Gao, S., and Chen, F., 2019. Preparation and Adsorption Properties of Biomass Activated Carbon from Ginger Stems. *Biomass Activated Carbon*. 4, 45-50.

Liu, N., Ma, W., Tao, J., Zhang, X., Su, J., Li, L., Yang, C., Gao, Y., Golberg, D., and Bando, Y., 2013. Cable-Type Supercapacitors Of Three-Dimensional Cotton Thread Based Multi-Grade Nanostructures For Wearable Energy Storage. *Advanced Material*. 25, 4925–4931.

Liu, Q.S., Zheng, T., and Li, N., 2010. Modifcation Of Bamboo-Based Activated Carbon Using Microwave Radiation And Its Efects On The Adsorption Of Methylene Blue. *Applied Surface Science .* 256, 3309–3315.

Liu, X., Zang, L., Xu, Y., Liu, Q., You, H., Chen, M., Yang, C., 2021. Activated Carbon Fiber Yarns With Birnessite-Type MnO_2 and Oxygen-Functional Groups For High-Performance Flexible Asymmetric Supercapacitors, *Diamond & Related Materials*. 115, 1-12.

Lundberg, D., 2013. *The Periodic Table Of Elements,* 1-2.

Luo, Y., Li, D., Chen, Y., Sun, X., Cao, Q., and Liu, X., 2019. The Performance of Phosphoric Acid In the Preparation of Activated Carbon-Containing Phosphorus Species From Rice Husk Residue. *Journal of Materials Science*. 54, 5008-5021.

Mahbubul, I.M., Saidur, R., and Amalina., 2013. Influence Of Particle Concentration And Temperature On Thermal Conductivity And Viscosity Of Al_2O_3/R14b Nanorefrigerant. *International Communications in Heat and Mass Transfer.* 43, 100-104.

Mahmood, M.A., and Baruah, S., 2011. Enhanced Visible Light Photocatal-Ysis By Manganese Doping Or Rapid Crystallization with ZnO Nanoparticles. *Mater. Chem. Phys.* 130, 531–535.

Marks-Block, T., Lake, F.K., and Curran, L.M., 2019. Effects Of Understory Fire Management Treatments On California Hazelnut, An Ecocultural Resource Of The Karuk and Yurok Indians In The Pacific Northwest. *Forest Ecology and Management. 450, 1-11.*

Mazlana, M.A.F., Uemuraa, Y., Yusupa, S., Elhassana, F., Uddinb, A., Hiwadab, A., and Demiyab, M., 2016. Activated Carbon From Rubber Wood Sawdust By Carbon Dioxide Activation. *Procedia Engineering.* 148, 530 – 537.

Meng, A., Yang, Z., Li, Z., Yuan, X., and Zhao, J., 2018. Nanochain Architectures Constructed By Hydrangea-Like MoS_2 Nano Flowers And Sic Nanowires: Synthesis, Mechanism And The Enhanced Electrochemical And Wide-Temperature Properties As An Additive-Free Negative Electrode For Supercapacitors. *Journal of Alloys and Compounds*. 746, 93–101.

Min-Min, Z., Deng-Jun, A.L., and Kai-Lu, L., 2011. Template Synthesis Of MnO_2/CNT Nanocomposite and Its Aplication In Rechargeable Lithium Batteries. *Transaction Of Nonferrous Metals Society*. 21, 2010-2014.

Minson, I.I., Zain, N.K.M., and Jose, R., 2019. Converson Oil Palm Kernel Shell Elektrodeposotion Mode On Rutawangium Oxide Supercapacitor Elektrode Aplication. *Waste Biomass Valorization.* 10, 2731-1740.

Mohammadi, N., Pourreza, K., Adeh, N.B., and Omidvar, M., 2021. Defective Mesoporous Carbon/MnO_2 Nanocomposite As An Advanced Electrode Material For Supercapacitor Application. *Journal Of Alloys and Compounds.* 883, 1-8.

Muktham, R., Suresh K., Bhargava, Bankupalli, S., and Ball, A.S., 2016. A Review on 1st and 2nd Generation Bioethanol Production-Recent Progress*. Journal of Sustainable Bioenergy Systems.* 6, 72-92.

Naderi, L., Shahrokhian, S., and Soavi, F., 2020. Fabrication of a 2.8 V High-Performance Aqueous Flexible Fiber-Shaped Asymmetric Micro-Supercapacitor Based on MnO_2/PEDOT:PSS-Reduced Graphene Oxide Nanocomposite Grown on Carbon Fiber Electrode. *Journal of Materials Chemistry A*. 8, 19588-19602.

Nahar, K.., Rahaman, M.H., Khan, G.M.A., Islam, M.K., and Al-Reza, S.M., 2021. Green synthesis of silver nanoparticles from Citrus sinensis peel extract and its antibacterial potential. *Asian Journal of Green Chemistry.* 5,135-150.

Najib, S., and Erdem, E., 2019. Current Progress Achieved In Novel Materials For Supercapacitor Electrodes: A Mini-Review. *Nanoscale Advances.* 8, 2817-2827.

Najjar, R., Awad, R., and Abdel-Gaber, A.M., 2018. Physical Properties of Mn_2O_3 Nanoparticles Synthesized by Co-precipitation Method at Different pH Values. *Journal of Superconductivity and Novel Magnetism*. 1-7.

Najmia, H., Mahreda, E.S., Mahyudin, R.P., and Kissinger., 2021. Pemanfaatan Arang Aktif Cangkang Kelapa Sawit Teraktivasi H_3PO_4 untuk Penurunan Kadar Besi (Fe), Mangan (Mn) dan Kondisi pH pada Air Asam Tambang Utilization. *EnviroScienteae*. 17, 30-37.

Nath, G., Singh, P.K., Dhapola, P.S., Dohare, S., Noor, I. M., Sharma, T., and Singh, A., 2022. Fabrication of Cornstarch Biopolymer-Derived Nano Porous Carbon As Electrode Material For Supercapacitor Application. *Biomass Conversion and Biorefnery*. 1, 1-8.

Nikoloski, P., 2016. Technology and Economic Development: Retrospective. *Journal of Process Management–New Technologies*. 4, 45-50.

Nugroho, M.A., 2011. *Rancang Bangun Sistem Sumber Daya Tag Aktif Rfid Berbasis Tenaga Surya Dengan Superkapasitor Sebagai Media Penyimpanan Energi*. Jakarta, Universitas Indonesia.

Nulu, V., 2021. Porous MnO_2/carbon Hybrid Material with Improved Electrochemical Performance. *The Korean Institute of Metals and Materials*. 59, 670-676.

Nurdiansyah, H., and Susanti, D., 2013. Perancangan Sensor Kelembaban Berbasis Kapasitor. *Jurnal Sains dan Seni Promits*. 1, 1-6.

Pang, M., Long, G., Jiang, S., Ji, Y., Han, W., Wang, B., and Xi, Y. 2015. One Pot Low-Temperature Growth Of Hierarchical MnO_2 Nanosheets On Nickel Foam For Supercapacitor Applications. *Electrochimica Acta*. 161, 297–304.

Pang, S.C., Anderson, M.A., and Chapman, T.W., 2000. Novel Electrode Materials For Thin-Film Ultracapacitors: Comparison Of Electrochemical Properties Of Sol-Gel-Derived And Electrodeposited Manganese Dioxide. *Journal of The Electrochemical Society*. 147, 444–450.

Patabang, D., Arif, E., Jalaluddin, and Aziz, N., 2019. The Effect Of Adding Candlenut Shell Into The Low-Rank Coal On Combustion Performance. *Journal Of Mechanical Engineering Research & Developments (Jmerd)*. 42, 116-121.

Patil, B.S., and Kulkarni, K.S., 2012. Development Of High Surface Area Activated Carbon From Waste Materia. *International Journal Of Advanced Engineering Research And Studies*.1, 109-113.

Patsalas, P., and Logothetidis, S., 2002. Optical Performance Of Nanocrys-Talline Transparent Ceria Films. *Appl. Phys. Lett.* 81, 466–468.

Peng, Z, Han, X., Li, S., Al-Youbi, A.O., Bashammakh, A.S, El-Shahawi, M.S., and Leblanc, R.M., 2017. Carbon Dots: Biomacromolecule Interaction. Bioimaging And Nanomedicine. *Coordination Chemistry Reviews*. 347, 256-277.

Pina, A.C., Amaya, A., Marcuzzo, J.S., Rodrigues, A.C., Baldan, M.R., Tancredi, R., and Cuna, A., 2018. Supercapacitor Electrode Based on Activated Carbon Wool Felt. *Journal Of Carbon Reseach.* 4, 1-12.

Prataap, R.C., Arunachalm, R., Raj. R.P., Mohan, S., and Peter, L., 2018. Effect Of Electrodeposition Modes On Ruthernium Oxide Electrodes Fpr Supercapacitor. *Current Applied Physics.*18-1143-1148.

Raj, B.G.S., Asiri, A.M, Qusti, A.H, Wu, J.J., and Anandan, S., 2014. Sonochemically Synthesized MnO_2 Nanoparticles As Electrode Material For Supercapacitors. *Ultrasonics Sonochemistry.* 21, 1933–1938.

Rajput, S., Kumar, D., and Agrawal, V., 2020. Green Synthesis of Silver Nanoparticles Using Indian Belladonna Extract and Their Potential Antioxidant, Anti-Inflammatory. *Anticancer and Larvicidal Activities*. *Plant Cell Reports.* 39, 921-939.

Rasdiansyah, Darmadi, dan Supardan, M.D., 2014. Optimasi Proses Pembuatan Karbon Aktif dari Ampas Bubuk Kopi gunakan Aktivator $ZnCl_2$. *Jurnal Teknologi dan Industri Pertanian Indonesia*. 3, 55-58.

Rashidi, N.A., and Yusup, S., 2017. A Review On Recent Technological Advancement In The Activated Carbon Production From Oil Palm Wastes. *Chem. Eng. J.* 314, 277–290.

Rawal, S., Joshi, S., and Kumar, Y., 2018. Synthesis and Characterization Of Activated Carbon From The Biomass Of Saccharum Bengalense For Electrochemical Supercapacitors. Synthesis and Characterization Of Activated Carbon From The Biomass Of Saccharum Bengalense For Electrochemical Supercapacitors. *Journal of Energy Storage*. 20, 418-426.

Rohmah, P.T., dan Redjeki, A.S., 2014. Pengaruh Waktu Karbonisasi Pada Pembuatan Karbon Aktif Berbahan Baku Sekam Padi dengan Aktivator KOH. *Konversi*. 3, 19-27.

Rosalina, Rochaeni,H., Lestari, S.P., Tedja, T., Riani, E., and Sugiarti, S., 2018. The Influence Of Phosphoric Acid Activation Of Carbon From Bintaro Fruit (Cerbera Odollam Gaertn) On The Adsorption of Chromium In Various Conditions Of pH. *International Journal Of Chemical Studies.* 6, 443-448.

Roy, S.H., Mollah, M.Y., Islam, M., and Susan, A.B.H., 2018. Poly(vinyl alcohol) MnO_2 nanocomposite flms as UV-shielding materials. *Polym. Bull.* 5, 1-15.

Sanchez-Lainez, J., Zornoza, B., Friebe, S., Caro, J., Cao, S., Sabetghadam, A., Seoane, B., Gascon, J., Kapteijn, F., Le Guillouzer, C., Clet, G., Daturi, M., Tellez, J.C., and Coronas, J., 2016. Influence of Zif^{-8} Particle Size In The Performance Of Polybenzimidazole Mixed Matrix Membranes For Precombustion CO_2 Capture And Its Validation Through Interlaboratory Test. *Journal Of Membrane Science*. 515, 45–53.

Sani, 2011. Pembuatan Karbon Aktif dari Tanah Gambut. *Jurnal Teknik Kimia*. 5, 400-406.

Sanni, E.S., Emetere, M.E., Odigure, J.O., Efeovbokhan, V.E., Agboola, O., and Sadiku, E.R., 2017. Determination Of Optimum Conditions For The Production Of Activated Carbon Derived From Separate Varieties Of

Coconut Shells. *International Journal of Chemical Engineering* . 3, 1–16.

Sathiya, M., Prakash, A.S., Ramesha, K., Tarascon, J.M., and Shukla, A. K., 2011. $V_2O_5^-$ Anchored Carbon Nanotubes For Enhanced Electrochemical Energy Storage. *Journal Of The American Chemical Society.* 133, 16291–16299.

Sekar, S., Lee, S., Vijayarengan, P., Kalirajan, K.M., Santhakumar, T., Sekar, S., and Sadhasivam, S., 2020. Upcycling of Wastewater via Effective Photocatalytic Hydrogen Production Using MnO_2 Nanoparticles-Decorated Activated Carbon Nanoflakes. *Nanomaterials.* 10,1-12.

Sekine, T., Narushima, H., Suzuki, T., Takayama, T., Kudo, H., Katsumura, Y., 2004. Technetium(IV) Oxide Colloids Produced By Radiolytic Reactions In Aqueous Pertechnetate Solution, Coll. *Surf:Physicochemical And Engineering Aspects*. 249, 105-109.

She, C., Wang, Z., Sun, F. Liu, P., and Zhang, L., 2020, Battery Aging Assessment For Real-World Electric Buse. Based On Incremental Capacity Analysis And Radial Basis Function Neural Network. *IEEE Transactions on Industrial Informatics.* 16, 3345–3354.

Shen, H., Zhang, Y., Song, X., Liu, Y.H., Wang, H., Duan, X., and Kong, F., 2018. Hydrothermal Synthesis Of Actiniaria-Shaped A-MnO_2/Activated Carbon And Its Electrochemical Performances Of Supercapacitor. *Journal Of Alloys And Compounds*. 1, 1-27.

Shen, L., Che, Q., Li, Q., and Zhang, X., 2013. Mesoporous $NiCo_2O_4$ Nanowire Arrays Grown on Carbon Textiles as Binder-Free Flexible Electrodes for Energy Storage*. Advanced Functional Materials.* 24, 2630-2637*.*

Sheng, E., Lu, Y., Tan, Y., Xiao, Y., Li, Z., Dai, Z., 2019. Oxidase-Mimicking Activity Of Ultrathin MnO_2 Nanosheets In A Colorimetric Assay Of Chlorothalonil In Food Samples. *Food Chemistry*. 331, 1-7.

Shi, Q., Zhang, J., Zhang, C., Nie, W., Zhang, B., Zhang, H., 2010. Adsoption Of Basic Violet 14 In Aqueous Solutions Usung $KMnO_4$-modified Activated Carbon. *Journal Of Colloid and Interface Science*. 343, 188-193.

Silva, Taís L., Cazetta, A. L., Souza, P.S.C., Zhang, T., Asefa, T., and Almeida, V.C., 2018., Mesoporous Activated Carbon Fibers Synthesized From Denim Fabric Waste: Efficient Adsorbents For Removal Of Textile Dye From Aqueous Solutions. *Journal Of Cleaner Production*. 171, 482-49*.*

Sing, K., Everett, D. H., Haul, R., Moscou, L., Pierotti, R.A., Rouguerol, J., and Siemieniewaka, T., 1985. Reporting Physiorption Data For Gas/Solidinterface With Special Refence To The Determination Of Surface Areaand Porosity*, Pure and Applied Chemistry*. 57, 603-619.

Souza, T.N.V.D., Vieira, M.G.A., Silva, M.G.C.D., Brasil, D.D.S.B., Carvalho, S.M.L.D., 2019. H_3PO_4-Activated Carbons Produced From Açai Stones And Brazil Nut Shells: Removal Of Basic Blue 26 Dye From Aqueous Solutions By Adsorption. *Environmental Science and Pollution Research*. 1, 1-15.

Suhas, Gupta, V.K., Carrott, P.J.M., Singh, R., Chaudhary, M., dan Kushwaha, S., 2016. Cellulose: A Review As Natural, Modified and Activated Carbon Adsorbent*. Bioresource Technology.* 216, 1066–1076.

Sun, C., Zhang, Y., Song, S., and Xue, D., 2013. Tunnel-dependent Supercapacitance of MnO_2: Effects of Crystal Structure. *Journal of Applied Crystallography.* 46, 1128–1135.

Sun, Q., Jiang, T., Zhao, G., and Shi, J., 2019. Porous Carbon Material Based On Biomass Prepared By Mgo Template Method And $ZnCl_2$ Activation Method As Electrode For High Performance Supercapacitor*, International Journal of Electrochemical Science.* 14, 1 – 14.

Surets, A.H., Kasih, J.A.F., dan Wisnanti, A., 2008. Pengaruh Suhu, Konsentrasi, Zat Activator dan Waktu Aktivasi Terhadap Daya Serap Karbon Aktif Dari Tempurung Kemiri. *Jurnal Teknik Kimia*. 15, 17-22.

Syarif, N., 2014. Performance Of Biocarbon Based Electrodes for Electrochemical Capacitor. *Energy Procedia*. 52, 18-25.

Tetra, O.N., Aziz, H., Emriadi, Ibrahim, S., dan Alif, A., 2018. Superkapasitoe Berbahan Dasar Karbon Aktif dan Larutan Ionik Sebagai Elektrolit. *Journal Zarah*. 6, 39-46.

Toupin, M., Brousse, T., and Belanger, D., 2004. Charge Storage Mechanism of MnO_2 Electrode Used in Aqueous Electrochemical Capacitor. *Chemistry of Materials*. 16, 3184-3190.

Tung , M.T., Luong, V.C., Trang, P.M., Tuyen, L.V., Thuy, H.T.B., and Wu, N., 2019. Activated Carbon With Hierarchical Porosity Derived From Biomass For Lithium Sulfur Batteries*, Vietnam Journal of Chemistry*. 57, 182-188.

Ullah, S., Yu, J.L., Huichao, I., Waheed, Y.B., Li, C., Zhu, C.S., Yu, J., Liu, H., Iqbal, W., Yang, B., Li, C., Zhu, C., and Xu, J., 2019. Fabrication Of MnO_2- Carbonized Cotton Yarn Derived Hierarchical Porous Active Carbon Flexible Supercapacitor Electrodes For Potential Applications In Cable-Type Devices*. Applied Surface Science*hen. 1, 1-32.

Van, K.L., and Thi, T.T.L., 2014. Activated Carbon Derived From Rice Husk by NaOH Activation and Application In Supercpacitor. *Progress In Natural Science Materials International*. 1,1-8.

Vangari, M., Pryor, T., and Jiang, J., 2013. Supercapacitors: Review Of Materials and Fabrication Methods. *Journal Of Energy Engineering*. 2, 72-79.

Verma A, Mehata M. S., 2016. Controllable Synthesis Of Silver Nano- Particles Using Neem Leaves And Their Antimicrobial Activity. *J Radiat Res Appl Sci* . 9,109–115.

Vytras, K., Svancara, I., and Metelka, R., 2009., Carbon Paste Elketrodes In Elektroanalytical Chemistry. *Journal Of The Serbian Chemical Society.* 74, 1021-1033.

Wachid, M.R., dan Setiarso, P., 2014. Pembuatan Elektroda Pasta Karbon Termodifikasi Bentonit untuk Analisis Ion Logam Tembaga(II) secara

Cyclic Voltammetry Stripping. *Prosiding Seminar Nasional Kimia*. Universitas Negeri Surabaya. Surabaya.

Wang, J.G., Kang, F., and Wei, B., 2015a. Engineering of MnO_2-based Nanocomposites For High Performance Supercapacitors. *Progress in Materials Science*. 74, 51–124.

Wang, J.W., Chen, Y., and Chen B.Z., 2015b. A Synthesis Method Of MnO_2/Activated Carbon Composite For Electrochemical Supercapacitors. *Journal Of The Electrochemical Society.* 162, A1654-A1661.

Wang, X.F., Wang, D.Z., and Liang, J., 2003. Performance Of Electric Double Layer Capacitors Using Active Carbons Prepared From Petroleum Coke By Koh And Vapor Re-Etching. *Journal of Materials Science and Technology.* 19, 265–269.

Wei, L., and Yushin, G. 2012. Nanostructured Activated Carbon From Natural Precursors For Electrical Double Layer Capacitors (Review). *Nano Energy*. 1, 552-565.

Wei, W., Cui, X., Chen, W., and Ivey, D.G., 2011. Manganese Oxide-Based Materials As Electrochemical Supercapacitor Electrodes. *Chemical Society Reviews*. 40,1697–1721.

Wen, Z.B., Qu, Q.T., and Gao, Q., 2009. An Activated Carbon With High Capacitance From Carbonization Of A Resorcinol-Formaldehyde Resin. *Electrochemistry Communications*. 11, 715–718.

White, R.J., Lugue, L., Budarin, V.L., Clark, J.H., Margurrie, D.J., 2009. Suppoted Metal Nanoparticles On Porous Materials, Method And Aplications. *Chemical Society Reviews*. 38, 481-494.

Xi, S., Zhu, Y., Yang, Y., and Liu., Y., 2017. Direct Synthesis of MnO_2 Nanorods on Carbon Cloth as Flexible Supercapacitor Electrode. *Journal of Nanomaterials*. 1, 1-8.

Xie, B., and Zhou, Y., 2019. Enhanced Capacitive Performance Of Activated Carbon Paper Electrode Material. *Journal Of Material.* 34, 2472-2481.

Xu, J.C., Xin, P.H., Han, Y.B., Wang, P.F., Jin, H.X., Jin, D.F., Peng, X.L., Hong, Li, J., Ge, H.L., Zhu, Z.W., and Wang, X.Q. 2014. Response And Adsorptive Properties For Methylene Blue Of $CoFe_2O_4$/Co_xFe_y/Activated Carbon Magnetic Composites. *Journal Of Alloys and Compounds.* 617, 622–626.

Yakout, S., and El-Deen, G.S., 2016. Characterization Of Activated Carbon Prepared By Phosphoric Acid Activation Of Olive Stones. *Arab J Che.* 9, S1155–S1162.

Yang, G., dan Park S.J., 2018. MnO_2 And Biomass-Derived 3D Porous Carbon Composites Electrodes For High Performance Supercapacitor Applications. *Journal of Alloys and Compound*. 1, 1-35.

Yang, X., Wang, Q., Lai, J., Cai, Z., Lv, J., Chen, X., Chen,Y., Zheng, X., Huang, B., and Lin, F., 2020, Nitrogen-Doped Activated Carbons Via Melamine-Assisted NaOH/KOH/Urea Aqueous System For High

Performance Supercapacitors. *Materials Chemistry and Physics.* 250, 1-8.

Yuan, B., Lu, M.; Eskridge, K.M., Isom, L.D., and Hanna, M.A., 2018. Extraction, Identification, and Quantification Of Antioxidant Phenolics From Hazelnut (*Corylus Avellana L.*) Shells. *Food Chemistry*. 244, 7–15.

Yuliusmad and Afifah, T.M., 2019. Production Of Palm Shell Based Activated Carbon By Two Stage Phosphoric Acid Impregnation and Physical Activation. *Materials Science And Engineering*. 1173, 1-7.

Yunus, Z.M., Al-Gheethi, A., Othman, N., Hamdan, R., Ruslan, N.N., 2020. Removal Of Heavy Metals From Mining Effluents In Tile And Electroplating Industries Using Honeydew Peel Activated Carbon: A Microstructure And Techno-Economic Analysis. *Journal Of Cleaner Production*. 251,1-13.

Zakir, M., and Sekine, T., 2009. Oxidation Reaction of $Tc(IV)O_2.nH_2O$ Nanocolloid Induced by Ultrasonic Wave. *Indo. Chimica Acta.* 2, 46-47.

Zakir, M., and Sekine, T., 2010. Sonolytic Oxidation of $Tc(IV)O_2.nH_2O$ Nanoparticles to Tc(VII)O in Aqueous Solution. *Atom Indonesia*. 36, 17-22.

Zakir, M., Sekine, T., Takayama, T., Kudo, H., Lin, M., Katsumura, Y., 2005. Technetium(IV) Oxide Colloids And The Precursor Produced By Bremstrahlung Irrradiation Of Aqueous Pertechnetate Solution, *Journal of Nuclear and Radiochemical Sciences.* 6, 243-247.

Zakir, M., Budi, P., Raya, I., Wulandari, R., and Sobrido, A.B.J., 2018. Determination of Specific Capacitance of Modified Candlenut Shell Based Carbon as Electrode Material for Supercapacitor. *Journal of Physics: Conference* Series. 979, 1-7.

Zakir, M., Fauziah, S., and Sumpala, G.T., 2019. Adsorption Of Chromium Ions By Candlenut Shell Based Carbon Activated With H_3PO_4. *Journal Of Physics: Conference Series*. 1341, 1-7.

Zeppa, G., Belviso, S., Bertolino, M., Cavallero, M.C., Bello, B.D., Ghirardello, D., Giordano, M., Giorgis,M. Grosso, R., Rolle, L and Gerbi, V., 2014. The Effect Of Hazelnut Roasted Skin From Different Cultivars On The Quality Attributes, Polyphenol Content and Texture Of Fresh Egg Pasta. *Journal of the Science of Food and Agriculture*. 95, 1678–1688.

Zhang, J., Chena , Y., Tana, J., and Sanga, H., 2016. The Sinthesis Of Rhodium/ Carbon Dots Nanoarticles And Its Hydro/Genation Application. *Applied Surface Science.* 396, 1-43.

Zhang, L., Zhang, X., Wang, J., Seveno, D., Fransaer , J., Locquet, J., and Seo J.W., 2021. Carbon Nanotube Fibers Decorated With MnO_2 For Wire-Shaped Supercapacitor. *Molecules.* 26, 1-19.

Zhang, X., Sun, X., Zhang, H., Zhang, D., and Ma, Z., 2012. Development Of Redox Deposition Of Birnesitte-Type MnO_2 On Activated Carbon As High-Performance Electrode For Hybrid Supercapacitors. *Material Chemistry and Physics*. 137, 290-296.

Zhang, P.Z., Zhao, X., and Li, P.J., 2015. Facile Synthesis of Nanostructured MnO_2 as Anode Materials for Sodium-Ion Batteries. *ChemNanoMat.* 3, 196-200.

Zhao, Q., Wang, X.Y., Xia, H., Liu, J., Wang, H., Gao, J., Zhang, S.Y., and Wang, X.Y., 2015. Design, Preparation and Performance Of Novel Three Dimensional Hierarchically Porous Carbon For Supercpacitors. *Electrochimica Acta.* 173, 566-567.

Zhou, Y., Li, J., Hu, S., Qian, G., Shi. J., Zhao, S., Wang, Y., Wang, C., and Lian, J., 2022. Sawdust-Derived Activated Carbon with Hierarchical Pores for High-Performance Symmetric Supercapacitors. *Nanomaterials.* 12, 1-10.

Zhu, J., Shi, W., Xiao, N., Ruia, X., Tan, H., Lu, X., Hng, H.H., Ma, J., Yan, Q., 2012. Oxidation Etching Preparation of MnO_2 Tubular Nanostructures for High-Performance Supercapacitors. *ACS Applied Materials & Interfaces*. 4, 2769–2774.

Zubir, M.H.M., and Zain, M.A.A., 2020. Twigs-Derived Activated Carbons Via H3PO4/ZnCl2 Composite Activation for Methylene Blue and Congo Red Dyes Removal. Scientific Reports. 1, 1-17.

Lampiran 1. Skema Alur Penelitian

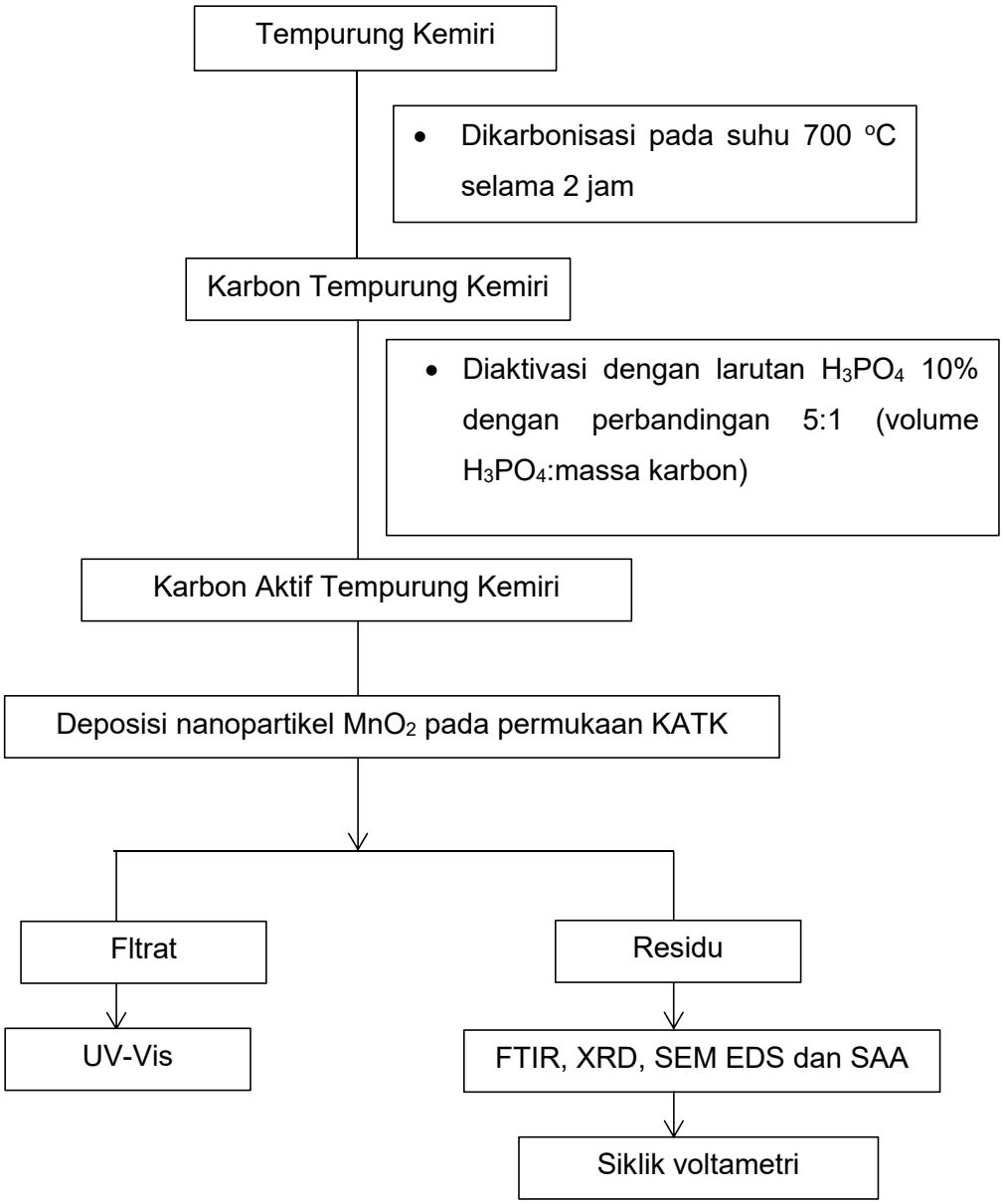

Lampiran 2. Skema Kerja Preparasi dan Karbonisasi Sampel

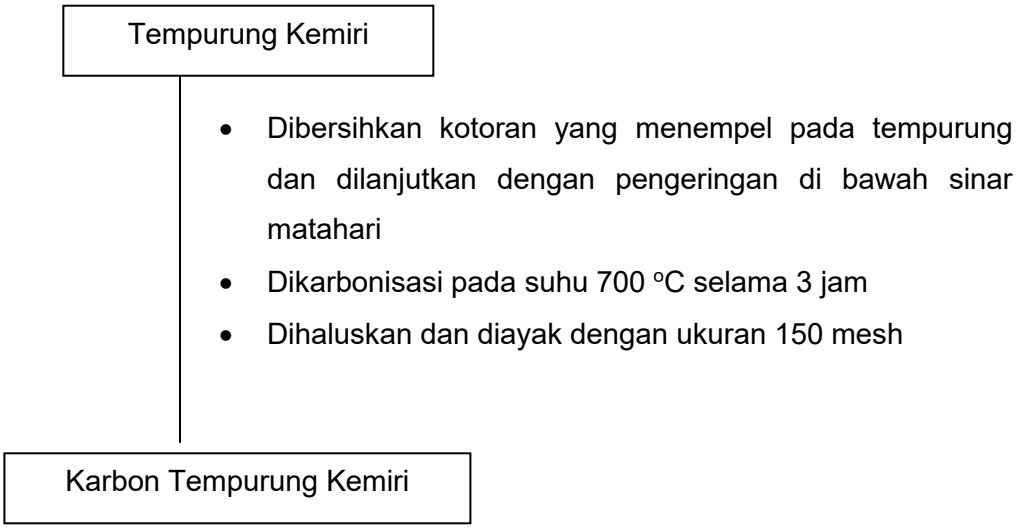

Lampiran 3. Skema Kerja AktivasiSampel

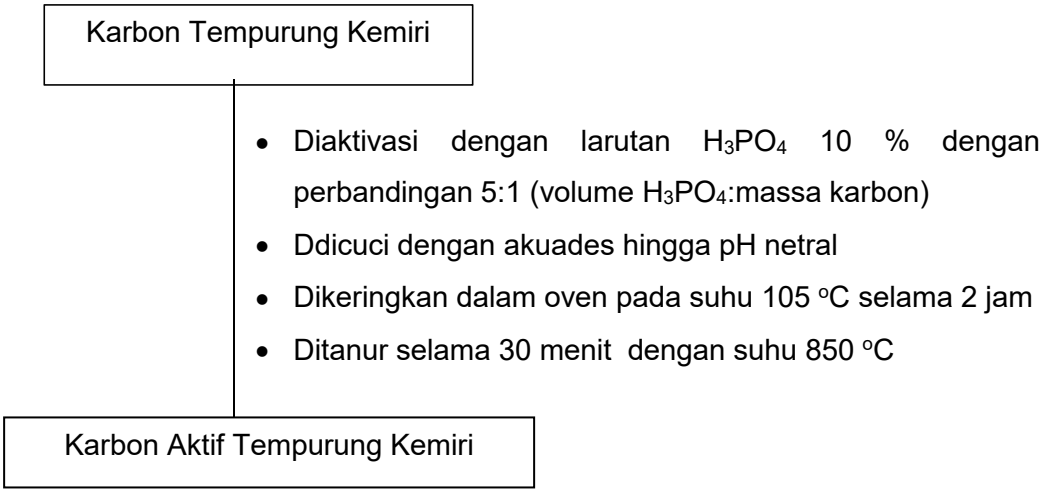

Lampiran 4. Skema pengaruh Massa KATK Terhadap pembentukan Nanopartikel MnO_2

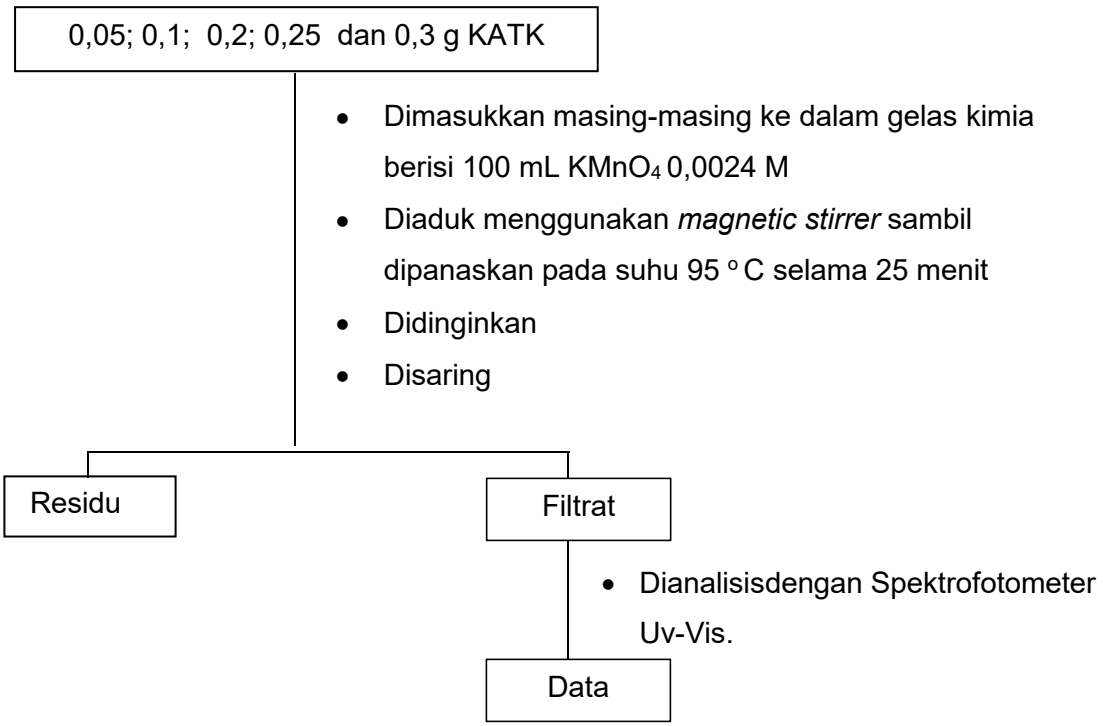

Lampiran 5. Skema Pengaruh Konsentrasi $KMnO_4$ Terhadap pemebentukan Nanopartikel MnO_2

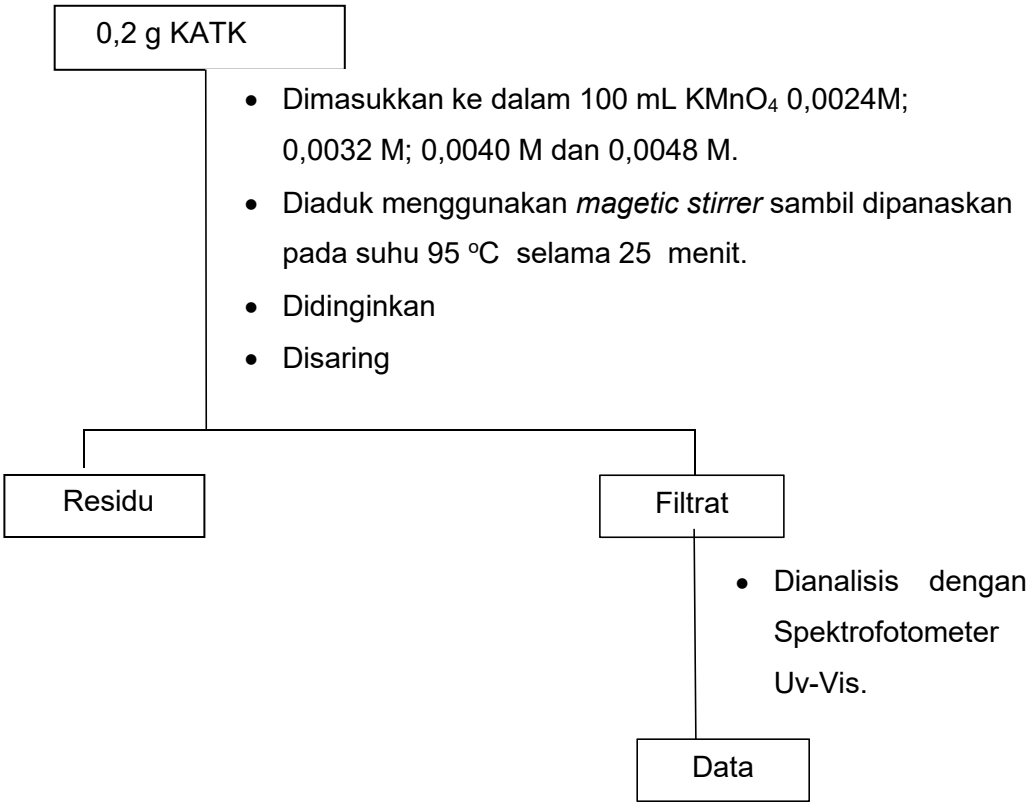

Lampiran 6. Skema Pengaruh pH Terhadap Pembentukan Nanopartikel MnO_2

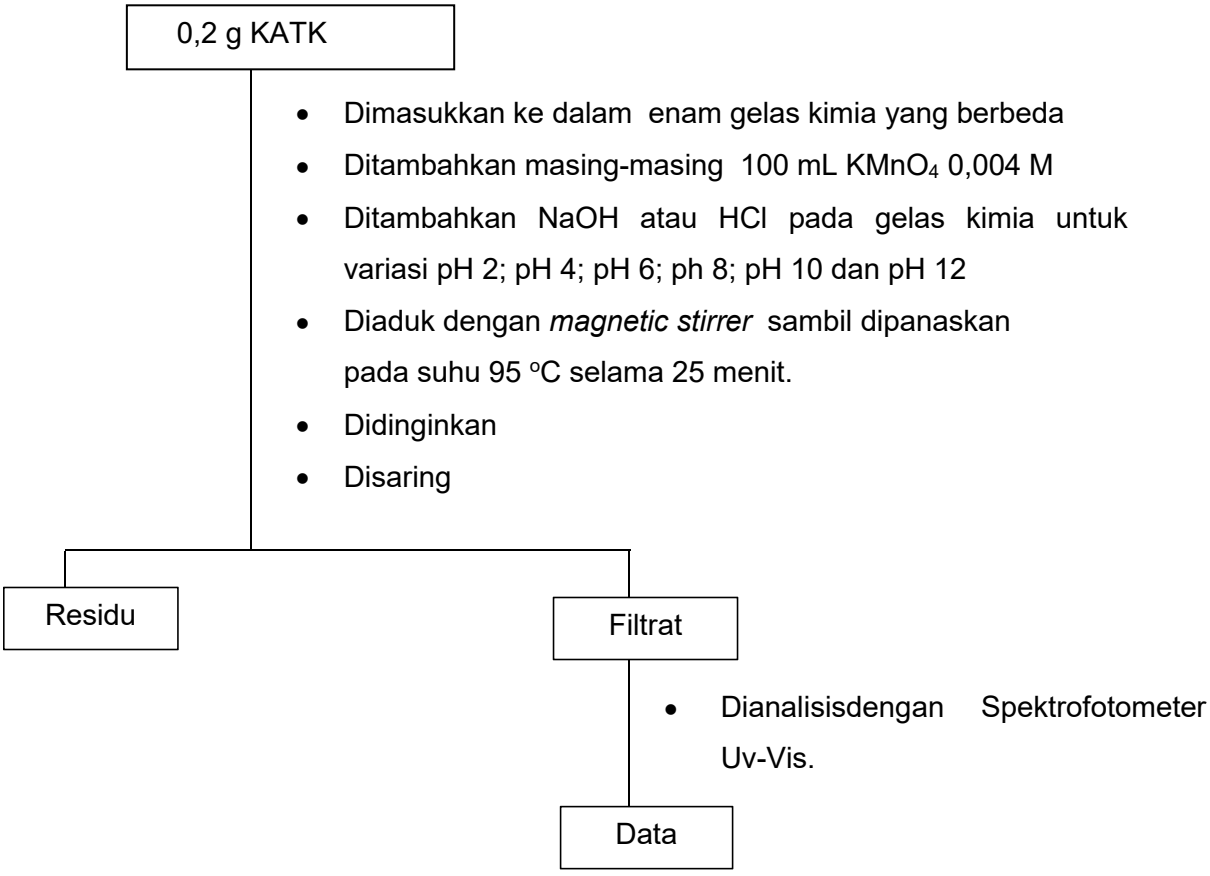

Lampiran 7. Skema Pengaruh Suhu Terhadap Pembentukan Nanopartikel MnO_2

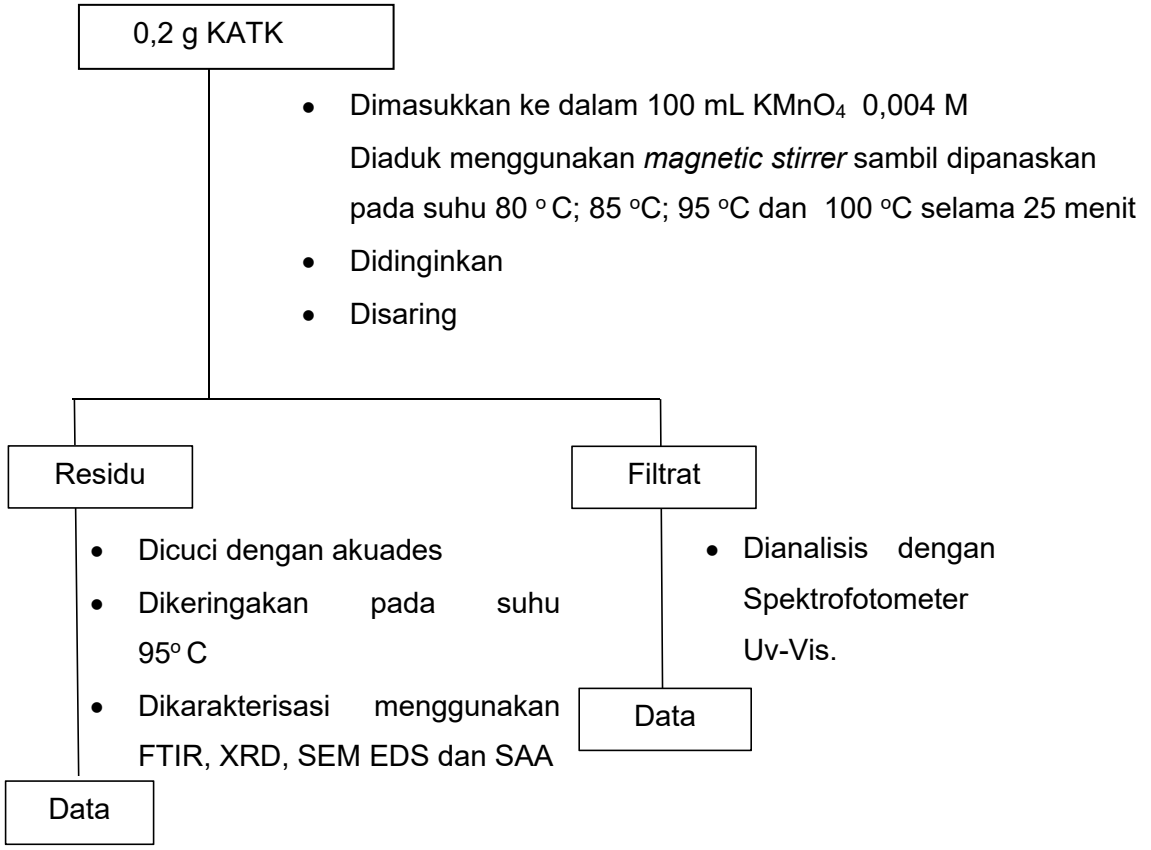

Lampiran 8. Skema Kerja Analisis Gugus Fungsi dengan Titrasi Boehm

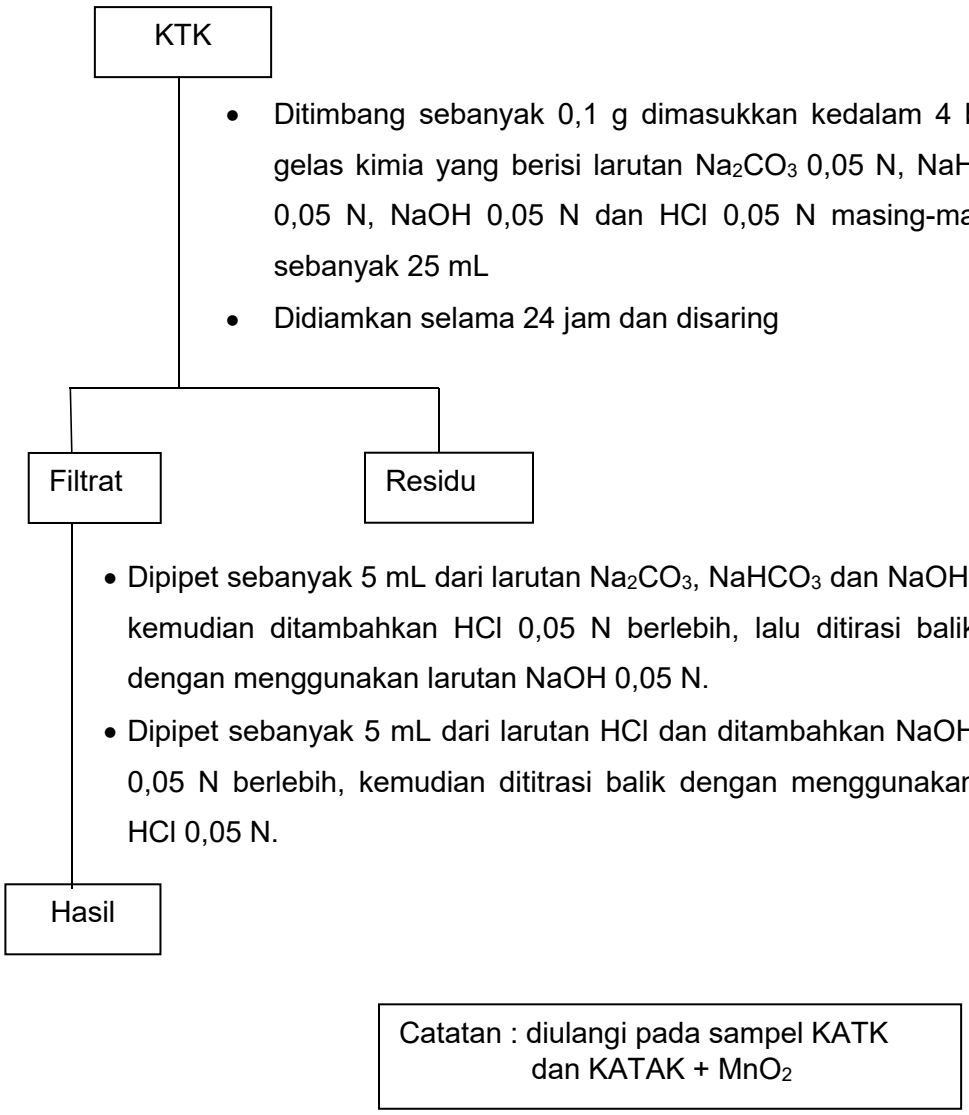

Lampiran 9. Skema Pembuatan Elektroda

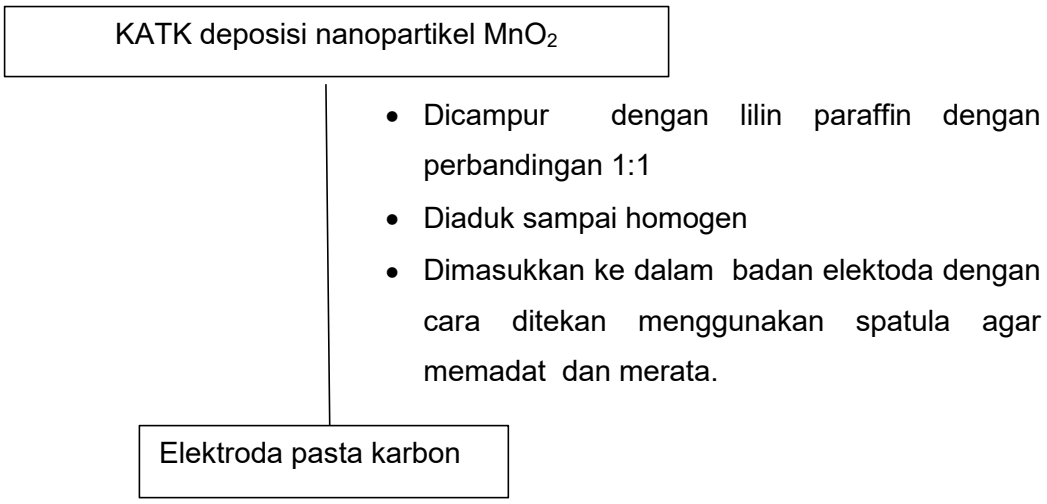

Lampiran 10. Pengukuran Nilai Kapasitansi Spesik

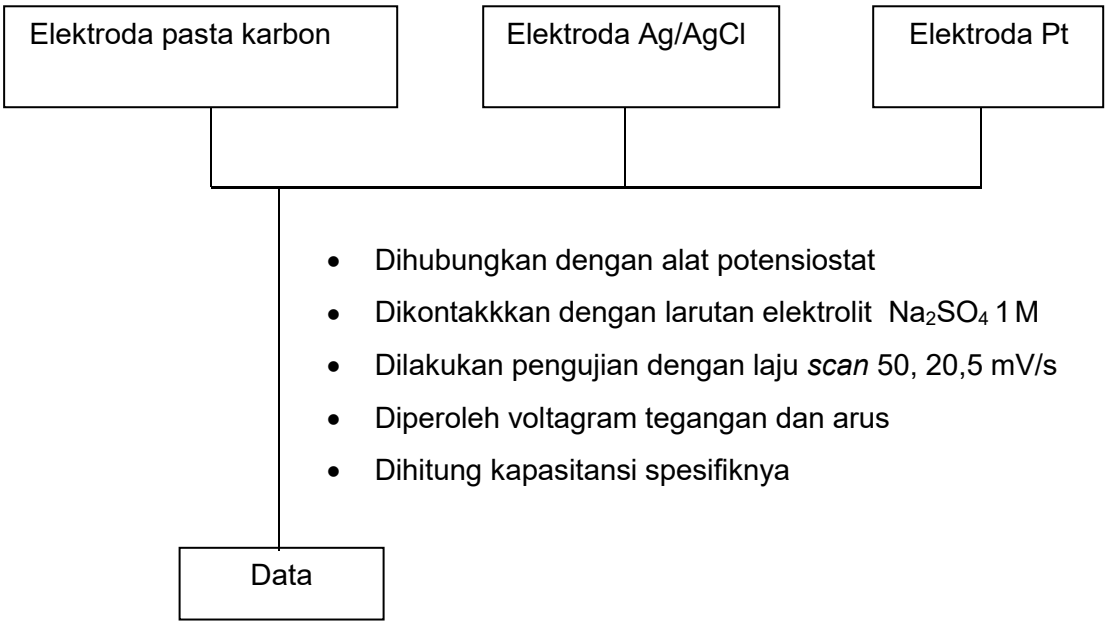

Lampiran 11. Perhitungan Pembuatan Larutan Pereaksi

2.1..Pembuatan Larutan H_3PO_4 10% dari H_3PO_4 85%

$V_1 \times M_1 = V_2 \times M_2$

$V_1 \times 85\% = 250\ mL \times 10\%$

$V_1 = 73.5\ mL$

2.2..Pembuatan Larutan Na_2CO_3 0,05 N

gram = L × N × BE

gram = 0,25 L × 0,05 N × 106 g/eq = 1,3250 gram

2.3..Pembuatan Larutan $NaHCO_3$ 0,05 N

gram = L × N × BE

gram = 0,25 L × 0,05 N × 84 g/eq = 1,0500 gram

2.4..Pembuatan Larutan NaOH 0,05 N

gram = L × N × BE

gram = 0,25 L × 0,05 N × 40 g/eq = 0,5000 gram

2.5..Pembuatan Larutan HCl 0,05 N

$$\mathrm{N} = \frac{\%\ \times \mathrm{bj}\ \times\ 10}{\mathrm{BE}}$$

$$\mathrm{N} = \frac{37 \times 1{,}19\ \mathrm{g/mL} \times 10}{36{,}5\ \mathrm{g/eq}}$$

$$\mathrm{N} = 12{,}06\ \mathrm{N}$$

$V_1 \times N_1 = V_2 \times N_2$

$V_1 \times 12{,}06\ N = 250\ mL \times 0{,}05\ N$

$V_1 = 1{,}03\ mL$

2.6..Pembuatan Larutan $Na_2B_4O_7$ 0,05 N

gram = L × N × BE

gram = 0,1 L × 0,05 N × 190,6 g/eq = 0,9530 gram

2.7..Pembuatan Larutan $H_2C_2O_4$ 0,05 N

gram = L × N × BE

gram = 0,1 L × 0,05 N × 63 g/eq = 0,3150 gram

2.8..Pembuatan Larutan Na_2SO_4 1 M

gram = L × M × BM

gram = 0,05 L × 1 M × 142,04 g/mol

gram = 7,1020 g

Lampiran 12. Perhitungan kadar koloid nanopartikel MnO_2

A= a.b.c (g/liter) atau A= ε. b. c (mol/liter)

	MnO_4^-	⟶	MnO_2
Mula-mula	A		
Bereaksi	C		C
Sisa	B		C

Ket: A : konsentrasi awal $KMnO_4$.

B : sisa konsentasi $KMnO_4$ setelah bereaksi dengan karbon.

C : Konsentrasi koloid MnO_2 (C = A - B).

a. Pengaruh massa KATK

1. Massa KTAK 0,005 g

$$c = \frac{0{,}875 \times 1}{2{,}40 \times 10^3}$$

$$c = 3{,}64583\ x10^{-4}$$

Kadar Koloid (%)

$$B = \frac{3{,}64583\ x10^{-4}}{0{,}0024} X100$$

$$B = 0$$

2. Massa KATK 0,01 g

$$c = \frac{0{,}670 \times 1}{9{,}6 \times 10^3}$$

$$c = 6{,}67917\ x10^{-5}$$

Kadar Koloid (%)

$$B = \frac{6{,}67917\ x10^{-5}}{0{,}0024} X100$$

$$B = 2{,}91\ \%$$

Absorbansi	Masssa KATK (gram)	Konsentrasi (c) MnO_2	Koloid nanopartikel MnO_2 (%)
0,875	0,005	0	0
0,67	0,10	$6,97917 X10^{-5}$	2,91
0,683	0,15	$7,11458 X 10^{5}$	2,94
0,722	**0,20**	$7,52083 X10^{-5}$	3,13
0,716	0,25	$7,45833 X 10^{-5}$	3,10
0	0,30	0	0

b. Pengaruh Konsentrasi $KMnO_4$

Absorbansi	Konsentrasi $KMnO_4$ (M)	Konsentrasi (c) MnO_2	Koloid nanopartikel MnO_2 (%)
0,722	0,0024	$7,52083 X 10^{-5}$	3,13
1,164	0,0032	$1,2125 X 10^{-4}$	3,79
1,537	0,004	$1,60104 X 10^{-4}$	4,00
1,22	0,0048	$127083 X 10^{-4}$	2,65

c. Pengaruh pH

Absorbansi	Ph	Konsentrasi (c) MnO_2	Koloid nanopartikel MnO_2 (%)
0,082	2	$8,54167 x 10^{-6}$	0,21
0,142	4	$1,47917 x 10^{-5}$	0,37
0,675	6	$7,03125 x 10^{-5}$	1,76
1,197	8	$1,24688 x 10^{-4}$	3,12
1,688	10	$1,75833 x 10^{-4}$	4,40
3	12	0	0

d. Pengaruh suhu

Absorbansi	Suhu (^{o})	Konsentrasi (c) MnO_2	Koloid nanopartikel MnO_2 (%)
1,352	80	$1,41 \times 10^{-4}$	3,52
1,485	85	$1,55 \times 10^{-4}$	3,87
1,534	90	$1,60 \times 10^{-4}$	4
1,688	95	$1,76 \times 10^{-4}$	4,4
1,853	100	$1,93 \times 10^{-4}$	4,82

Lampiran 13. Perhitungan Kadar Gugus Fungsi dengan Titrasi Boehm

a. Karbon Tempurung Kemiri (KTK)

- **Penentuan Kadar Asam kaboksilat**

No	V. Sampel (Vs) (mL)	V. Titran NaHCO3 (Vp) (mL)	N. NaHCO3	N. HCl	V. HCl (mL)	N. NaOH	V. NaOH (mL)	Massa Karbon (g)	n Carboxyl (meq/g)
1	25	5	0,05	0,0304	7	0,0558	1,2	0,1024	5,0894
2	25	5	0,05	0,0304	7	0,0558	1,3	0,1024	5,3618
3	25	5	0,05	0,0304	7	0,0558	1,1	0,1024	4,8169
Rata – rata									**5,0894**

$$n_{carboxylic} = \frac{\left[V_{NaHCO_3} N_{NaHCO_3} - (N_{HCl} V_{HCl} - N_{NaOH} V_{NaOH})\right] \frac{V_p}{V_s}}{w}$$

$$n_{carboxylic} = \frac{[5\ mL \times 0{,}05\ N - (0{,}03004\ N \times 7\ mL - 0{,}0558\ N \times 1{,}2\ mL)] \frac{25\ mL}{5\ mL}}{0{,}1024\ gram}$$

$$n_{carboxylic} = \frac{[0{,}25\ meq - 0{,}146\ meq] \frac{25\ mL}{5\ mL}}{0{,}1024\ gram} = 5{,}0894\ \frac{meq}{gram}$$

- **Penentuan Kadar Lakton**

No	V. Sampel (Vs) (mL)	V. Titran Na2CO3 (Vp) (mL)	N. Na2CO3	N. HCl	V.HCl (mL)	N. NaOH	V.NaOH (mL)	Massa Karbon (g)	n Lactone (meq/g)
1	25	5	0,05	0,0304	7	0,0558	1,1	0,1043	-0,3602
2	25	5	0,05	0,0304	7	0,0558	1,2	0,1043	-0,0927
3	25	5	0,05	0,0304	7	0,0558	1	0,1043	-0,6277
Rata- rata									**-0,3602**

$$n_{lactonic} = \frac{\left[V_{Na_2CO_3} N_{Na_2CO_3} - (N_{HCl} V_{HCl} - N_{NaOH} V_{NaOH})\right] \frac{V_p}{V_s}}{w} - n_{carboxylic}$$

$$n_{lactonic} = \frac{[5\ mL \times 0{,}05\ N - (0{,}0304\ N \times 7\ mL - 0{,}0558\ N \times 1{,}1\ mL)] \frac{25\ mL}{5\ mL}}{0{,}3178\ gram} - 5{,}0894\ \frac{meq}{gram}$$

$$n_{lactonic} = \frac{[0{,}25\ meq - (0{,}151\ meq)] \frac{25\ mL}{5\ mL}}{0{,}1043\ gram} - 5{,}0894\ \frac{meq}{gram}$$

$$n_{lactonic} = -\ 0{,}3602\ \frac{meq}{gram}$$

- **Penentuan Kadar Fenol**

No	V. Sampel (Vs) (mL)	V. Titran NaOH (Vp) (mL)	N. NaOH	N. HCl	V. HCl (mL)	N. NaOH	V. NaOH (mL)	Massa Karbon (g)	n Phenolic (meq/g)
1	25	5	0,0558	0,0304	7	0,0558	1	0,1012	1,3020
2	25	5	0,0558	0,0304	7	0,0558	1,1	0,1012	1,5777
3	25	5	0,0558	0,0304	7	0,0558	1	0,1012	1,3020
Rata –rata									**1,3939**

$$n_{phenolic} = \frac{[V_{NaOH}N_{NaOH} - (N_{HCl}V_{HCl} - N_{NaOH}V_{NaOH})]\frac{V_p}{V_s}}{w} - n_{carboxylic} - n_{lactonic}$$

$$n_{phenolic} = \frac{[5\ mL \times 0{,}0558N - (0{,}0304\ N \times 7\ mL - 0{,}0558\ N \times 1\ mL)]\frac{25\ mL}{5\ mL}}{0{,}1012\ gram} - 5{,}0894\ \frac{meq}{gram} - (-0{,}3602\ \frac{meq}{gram})$$

$$n_{phenolic} = \frac{[0{,}25\ meq - (0{,}2127\ meq - 0{,}0558\ meq)]\frac{25\ mL}{5\ mL}}{0{,}1012\ gram} - 5{,}0894\ \frac{meq}{gram} - (-0{,}3602\ \frac{meq}{gram})$$

$$n_{phenolic} = 1{,}3020\ \frac{meq}{gram}$$

- **Penentuan Kadar Basa Total**

No	V. Sampel (Vs) (mL)	V. Titran HCl (Vp) (mL)	N. HCl	N. NaOH	V. NaOH (mL)	N. HCl	V. HCl (mL)	Massa Karbon (g)	n total base (meq/g)
1	25	5	0,0304	0,0558	7	0,0304	8	0,1011	0,2211
2	25	5	0,0304	0,0558	7	0,0304	8,1	0,1011	0,3714
3	25	5	0,0304	0,0558	7	0,0304	8,2	0,1011	0,5217
Rata – rata									**0,3714**

$$n_{total\ base} = \frac{[\ V_{HCl}N_{HCl} - (N_{NaOH}V_{NaOH} - N_{HCl}V_{HCl})\ ]\ \frac{V_p}{V_s}}{w}$$

$$n_{total\ base} = \frac{[5\ mL \times 0.0304\ N - (0.0558\ N \times 7\ mL - 0.0304\ N \times 8\ mL)\ ]\ \frac{25\ mL}{5\ mL}}{0.1011\ gram}$$

$$n_{total\ base} = \frac{[0.152\ meq - (0.3906\ meq - 0.24312\ meq)\ ]\ \frac{25\ mL}{5\ mL}}{0.1011\ gram}$$

$$n_{total\ base} = \frac{[0.152\ meq - 0.14748\ meq\ ]\ \frac{25\ mL}{5\ mL}}{0.1001\ gram} = 0.2211\ \frac{meq}{gram}$$

b. Karbon Aktif Tempurung Kemiri (KATK)

- Penentuan Kadar Asam kaboksilat

No	V. Sampel (Vs) (mL)	V. Titran NaHCO3 (Vp) (mL)	N. NaHCO3	N. HCl	V. HCl (mL)	N. NaOH	V. NaOH (mL)	Massa Karbon (g)	n Carboxyl (meq/g)
1	25	5	0,05	0,0370	8	0,0558	3,8	0,1013	8,1955
2	25	5	0,05	0,0370	8	0,0558	3,8	0,1013	8,1955
3	25	5	0,05	0,0370	8	0,0558	4,5	0,1013	10,1234
Rata – rata									**8,8381**

- Penentuan Kadar Lakton

No	V. Sampel (Vs) (mL)	V. Titran Na2CO3 (Vp) (mL)	N. Na2CO3	N. HCl	V. HCl (mL)	N. NaOH	V. NaOH (mL)	Massa Karbon (g)	n Lactone (meq/g)
1	25	5	0,05	0,0370	8	0,0558	4	0,1021	0,4823
2	25	5	0,05	0,0370	8	0,0558	4,1	0,1013	0,8263
3	25	5	0,05	0,0370	8	0,0558	4,1	0,1013	-1,1017
Rata – rata									**0,0690**

- Penentuan Kadar Fenol

	V. Sampel (Vs) (mL)	V. Titran NaOH (Vp) (mL)	N. NaOH	N. HCl	V. HCl (mL)	N. NaOH	V. NaOH (mL)	Massa Karbon (g)	n Phenolic (meq/g)
1	25	5	0,0558	0,0370	8	0,0558	5	0,1017	4,2033
2	25	5	0,0558	0,0370	8	0,0558	5,1	0,1017	4,1336
3	25	5	0,0558	0,0370	8	0,0558	5,1	0,1017	4,1336
Rata – rata									**4,1568**

- Penentuan Kadar Basa Total

No	V. Sampel (Vs) (mL)	V. Titran HCl (Vp) (mL)	N. HCl	N. NaOH	V. NaOH (mL)	N. HCl	V. HCl (mL)	Massa Karbon (g)	n total base (meq/g)
1	25	5	0,0370	0,0558	8	0,0304	2,3	0,1027	-9,3234
2	25	5	0,0370	0,0558	8	0,0304	2,3	0,1027	-9,3234
3	25	5	0,0370	0,0558	8	0,0304	2,3	0,1027	-9,3234
Rata – rata									**-9,3234**

Lampiran 14. Perhitungan Kapasitansi Spesifik

1. Perhitungan Kapasitansi Spesifik KTK

***Scan rate* 50 mV/s**

$$C_s = \frac{(6{,}13\text{x } 10^{-4} - (-6{,}88 \text{ x } 10^{-7})\ A}{0{,}05\ V/_s \text{ x } 0{,}0523 \text{ gram}} = \frac{(6{,}13\text{x } 10^{-3})\ A}{0{,}05\ V/_s \text{ x } 0{,}0529 \text{ gram}} = 0{,}2188\ F/_g$$

***Scan rate* 10 mV/s**

$$C_s = \frac{(3{,}88\text{x } 10^{-4} - (-2{,}13 \text{ x } 10^{-4})\ A}{0{,}002\ V/_s \text{ x } 0{,}0529 \text{ gram}} = \frac{(-2{,}13\text{x } 10^{-4})\ A}{0{,}002\ V/_s \text{ x } 0{,}0529 \text{ gram}} = 0{,}5671\ F/_g$$

***Scan rate* 5 mV/s**

$$C_s = \frac{(9{,}38\text{x } 10^{-5} - (-6{,}88 \text{ x } 10^{-5})\ A}{0{,}005\ V/_s \text{ x } 0{,}0529 \text{ gram}} = \frac{(7{,}39\text{x } 10^{-3})\ A}{0{,}005\ V/_s \text{ x } 0{,}0529 \text{ gram}} = 0{,}6144\ F/_g$$

2. Perhitungan Kapasitansi Spesifik KATK

***Scan rate* 50 mV/s**

$$C_s = \frac{(1{,}29\text{x } 10^{-6} - (-1{,}23 \text{ x } 10^{-3})\ A}{0{,}05\ V/_s \text{ x } 0{,}0505 \text{ gram}} = \frac{(-1{,}23\text{x } 10^{-3})\ A}{0{,}05\ V/_s \text{ x } 0{,}0578 \text{ gram}} = 0{,}42605\ F/_g$$

***Scan rate* 20 mV/s**

$$C_s = \frac{(1{,}14\text{x } 10^{-6} - (-9{,}88 \text{ x } 10^{-4})\ A}{0{,}02\ V/_s \text{ x } 0{,}0578 \text{ gram}} = \frac{(9{,}89\text{x } 10^{-4})\ A}{0{,}02\ V/_s \text{ x } 0{,}0578 \text{ gram}} = 0{,}8552\ F/_g$$

***Scan rate* 5 mV/s**

$$C_s = \frac{(-3{,}18\text{x } 10^{-6} - (-3{,}02 \text{ x } 10^{-3})\ A}{0{,}005\ V/_s \text{ x } 0{,}0505 \text{ gram}} = \frac{(3{,}02\text{x } 10^{-3})\ A}{0{,}005\ V/_s \text{ x } 0{,}0578 \text{ gram}} = 10{,}4388\ F/_g$$

3. Perhitungan Kapasitansi Spesifik KATK+MnO_2

***Scan rate* 50 mV/s**

$$C_s = \frac{(2{,}34\text{x } 10^{-5} - (-1{,}73 \text{ x } 10^{-2})\ A}{0{,}05\ V/_s \text{ x } 0{,}0677 \text{ gram}} = \frac{(1{,}73\text{x } 10^{-2})\ A}{0.005\ V/_s \text{ x } 0{,}0587 \text{ gram}} = 5{,}6253\ F/_g$$

***Scan rate* 20 mV/s**

$$C_s = \frac{(2{,}76\text{x } 10^{-5} - (-1{,}93 \text{ x } 10^{-2})\ A}{0{,}005\ V/_s \text{ x } 0{,}0677 \text{ gram}} = \frac{(1{,}93\text{x } 10^{-2})\ A}{0{,}005\ V/_s \text{ x } 0{,}0677 \text{ gram}} = 14{,}2375\ F/_g$$

***Scan rate* 5 mV/s**

$$C_s = \frac{(3{,}19\text{x } 10^{-2} - (-3{,}15 \text{ x } 10^{-5})\ A}{0{,}005\ V/_s \text{ x } 0{,}0677 \text{ gram}} = \frac{(-1{,}00044\text{x } 10^{-6})\ A}{0{,}005\ V/_s \text{ x } 0{,}0677 \text{ gram}} = 94{,}1847\ F/_g$$

a. Elekrolit Na_2SO_4 1 M

Sampel	***Scan rate*** **(V/s)**	**I_c** **(A)**	**I_d** **(A)**	**Massa karbon (gram)**	**Kapasitansi spesifik (F/g)**
KTK	0,05	$1,29x\ 10^{-6}$	$-6,88 \times 10^{-7}$	0,0529	0,2188
	0,02	$1,14x\ 10^{-6}$	$-9,88 \times 10^{-4}$	0,0529	0,5671
	0,005	$9,38x\ 10^{-5}$	$-6,88 \times 10^{-5}$	0,0529	0,6144
KTAK	0,05	$1,29x\ 10^{-6}$	$-1,23 \times 10^{-3}$	0,0578	0,4260
	0,02	$1,14x\ 10^{-6}$	$-9,88 \times 10^{-4}$	0,0578	0,8552
	0,005	$-3,18x\ 10^{-6}$	$-3,02 \times 10^{-3}$	0,0578	10,4388
KTAK + MnO_2	0,05	$2,34x\ 10^{-5}$	$-1,73 \times 10^{-2}$	0,0512	5,6253
	0,02	$2,76x\ 10^{-5}$	$-1,93 \times 10^{-2}$	0,0677	14,2375
	0,005	$3,19x\ 10^{-2}$	$-3,15 \times 10^{-5}$	0,0677	94,1847

Lampiran 15. Dokumentasi

Tempurung kemiri

Tempurung kemiri dikarbonisasi

Karbon tempurung kemiri

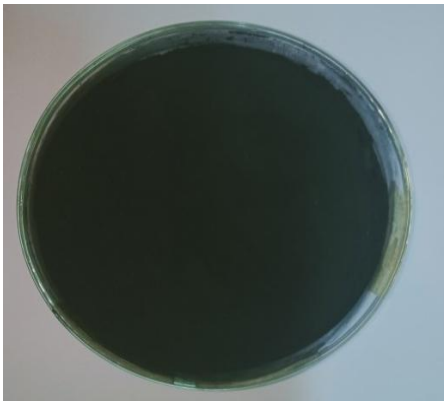

Karbon tempurung kemiri
150 *mesh*

Aktivasi karbon tempurung kemiri dengan H_3PO_4

Penetralan karbon aktif tempurung kemiri

Karbon aktif tempurung Kemiri

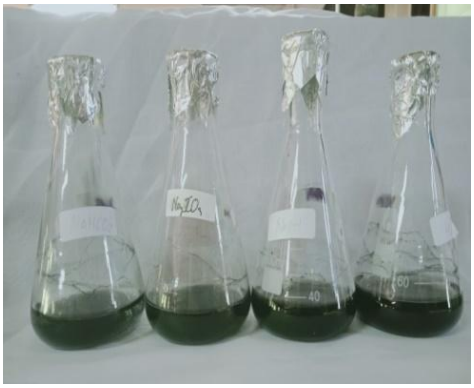

Perendaman sampel untuk titrasi Boehm

Hasil titrasi Boehm

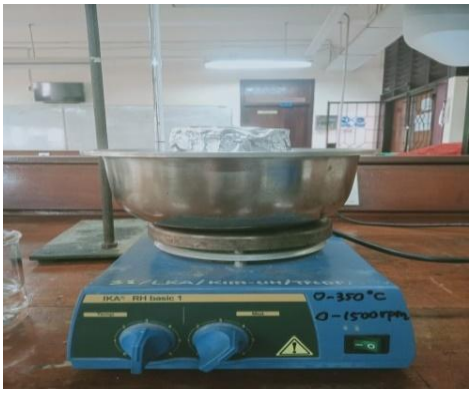

Deposisi nanopartikel MnO_2

Filtrat sebelum dan sesudah deposisi MnO_2

Penyaringan filtrat hasil deposisi

KATK + MnO_2

Pembuatan pasta karbon

Pembutan Elektroda

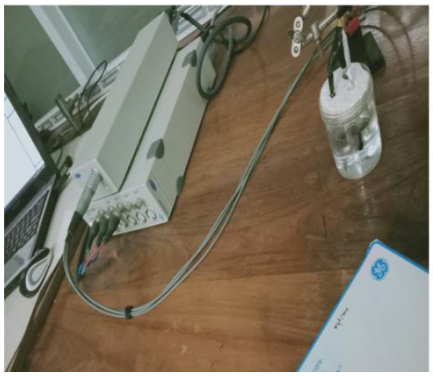

Pengukuran Kapasitansi

Lampiran 16. DATA FTIR

1. KTK

SHIMADZU

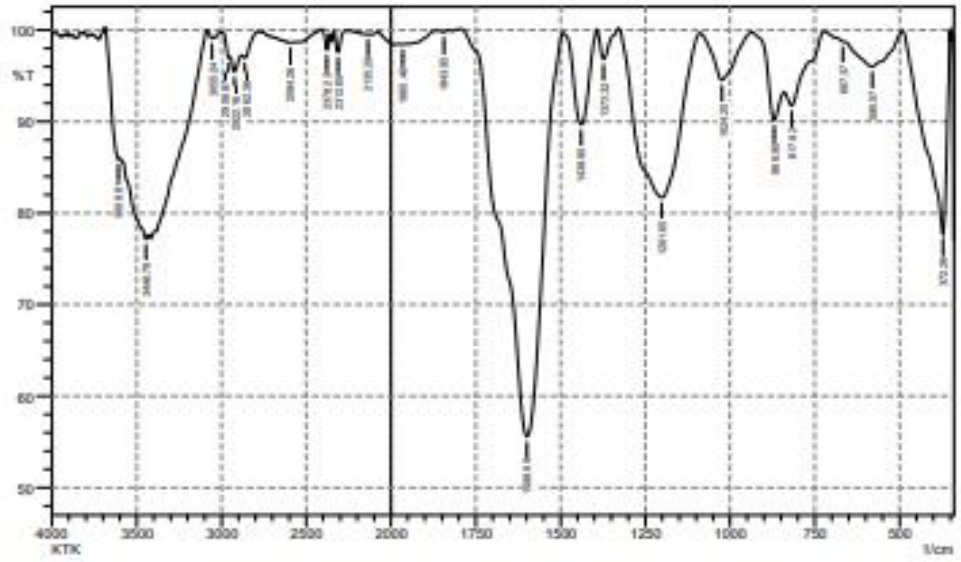

No.	Peak	Intensity	Corr. Intensity	Base (H)	Base (L)	Area	Corr. Area
1	372.26	77.773	21.068	491.85	352.97	7.287	6.845
2	580.57	96.018	3.281	663.51	493.78	1.975	1.47
3	667.37	98.742	0.04	723.31	685.44	0.177	0.002
4	817.82	91.759	2.643	839.03	723.31	2.373	0.597
5	869.9	90.153	5.042	935.48	840.96	2.061	0.668
6	1024.2	94.537	5.17	1087.85	937.4	1.811	1.622
7	1201.65	81.698	18.218	1327.03	1089.78	12.083	12.009
8	1373.32	96.848	3.214	1392.61	1328.95	0.389	0.417
9	1438.9	89.688	10.097	1490.97	1394.53	2.275	2.182
10	1598.99	55.583	44.261	1795.73	1492.9	30.125	30
11	1843.95	99.784	0.189	1857.45	1828.52	0.014	0.011
12	1965.46	98.429	0.076	1977.04	1951.96	0.168	0.004
13	2135.2	99.525	0.057	2245.14	2121.7	0.165	0.026
14	2312.65	97.599	2.309	2335.8	2264.43	0.321	0.295
15	2378.23	97.839	1.896	2411.02	2360.87	0.195	0.155
16	2594.26	98.631	0.3	2785.21	2546.04	0.941	0.178
17	2862.36	96.973	0.777	2881.65	2785.21	0.716	0.093
18	2922.16	95.463	1.652	2949.16	2881.65	1.085	0.234
19	2956.87	96.983	0.514	2995.45	2949.16	0.341	0.017
20	3055.24	99.083	0.444	3086.11	3037.89	0.127	0.049
21	3446.79	77.173	1.15	3581.81	3433.29	14.125	0.894
22	3638.81	85.921	1.345	3687.9	3601.1	3.369	0.558

Comment;
KTK

Date/Time; 7/22/2021 4:12:08 PM
No. of Scans;
Resolution;
Apodization;

2. KATK

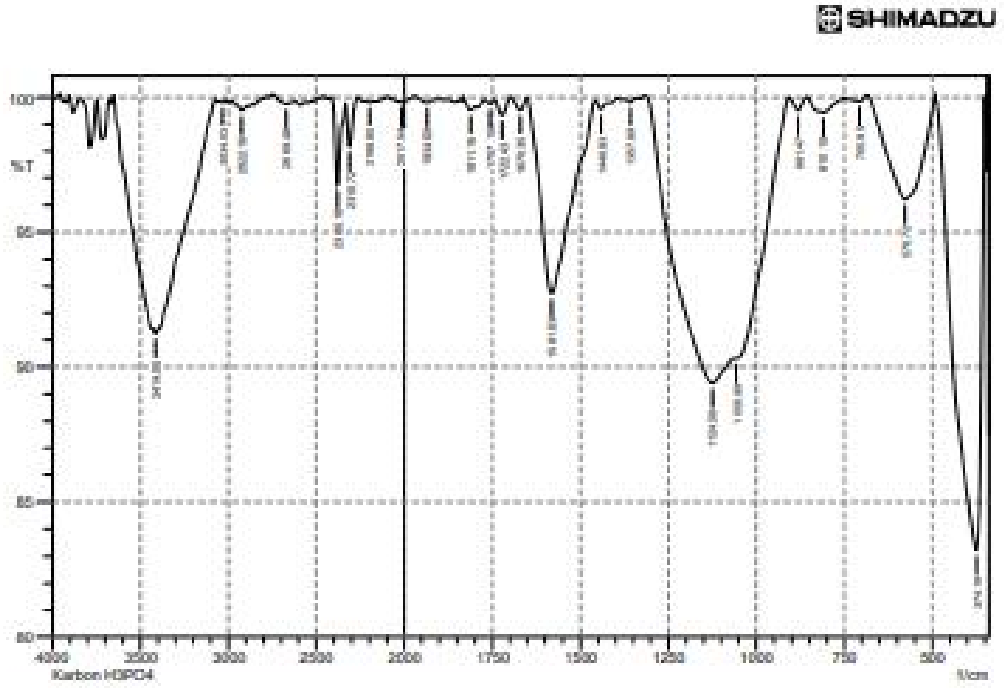

No.	Peak	Intensity	Corr. Intensity	Base (H)	Base (L)	Area	Corr. Area
1	374.19	83.231	16.687	491.85	351.04	6.545	6.526
2	576.72	96.208	3.815	584.73	493.78	1.845	1.868
3	705.98	99.852	0.185	748.38	684.73	0.022	0.026
4	810.1	99.435	0.551	858.32	752.24	0.152	0.144
5	881.47	99.499	0.5	906.54	858.32	0.056	0.055
6	1058.99	90.325	9.124	1058.92	908.47	3.716	3.441
7	1124.5	89.4	3.43	1313.52	1058.92	8.573	2.962
8	1357.89	99.811	0.137	1375.25	1340.53	0.017	0.009
9	1440.83	99.541	0.293	1458.18	1421.54	0.049	0.022
10	1581.63	92.722	7.213	1651.07	1458.18	3.165	3.1
11	1670.35	99.511	0.477	1697.36	1653	0.05	0.049
12	1722.43	99.332	0.624	1743.65	1697.36	0.069	0.061
13	1757.15	99.74	0.171	1772.58	1743.65	0.021	0.01
14	1811.16	99.511	0.268	1834.3	1783.73	0.056	0.025
15	1934.6	99.794	0.102	1969.32	1897.05	0.032	0.027
16	2017.54	99.623	0.207	2098.55	1969.32	0.051	0.067
17	2198.85	99.805	0.081	2220.07	2169.92	0.036	0.006
18	2310.72	98.177	1.681	2333.87	2288.36	0.25	0.219
19	2380.16	96.768	3.137	2414.88	2333.87	0.463	0.424
20	2669.46	99.74	0.166	2746.63	2634.76	0.069	0.05
21	2922.16	99.494	0.229	2947.23	2864.29	0.136	0.038
22	3034.03	99.804	0.085	3049.46	3014.74	0.024	0.005
23	3414	91.236	8.944	3553.18	3392.79	8.333	1.294

Comment;
Karbon H3PO4

Date/Time: 6/28/2021 12:16:45 PM
No. of Scans;
Resolution;
Apodization;

3.KATK+MnO_2

SHIMADZU

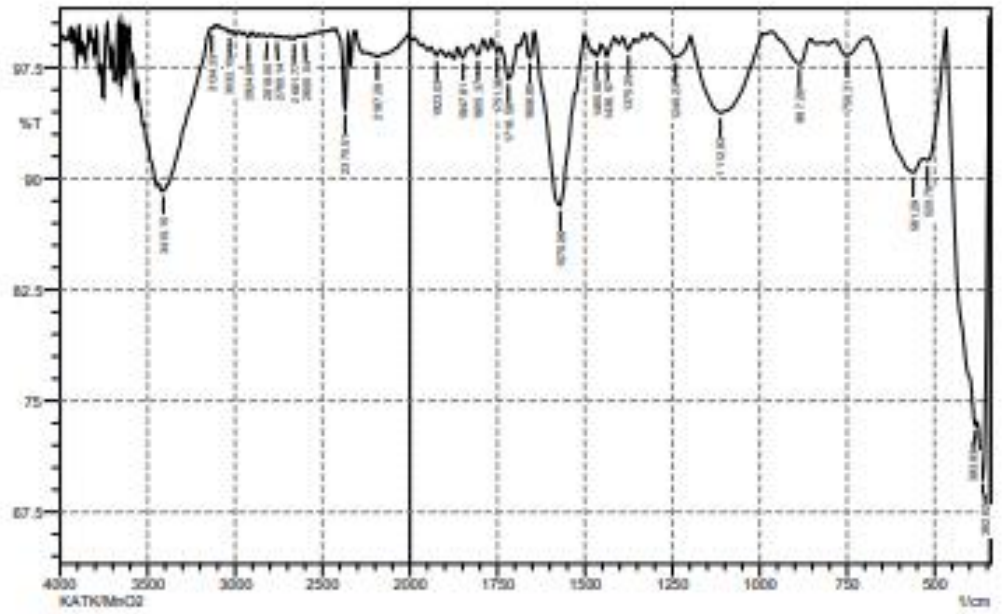

No.	Peak	Intensity	Corr. Intensity	Base (H)	Base (L)	Area	Corr. Area
1	382.62	69.75	13.931	376.12	343.33	3.696	1.499
2	383.83	73.363	1.891	486.77	378.05	7.773	1.742
3	520.78	91.234	1.432	530.42	488.7	1.627	0.427
4	561.29	90.415	2.425	690.52	532.35	4.625	1.332
5	750.31	98.321	1.103	785.03	692.44	0.453	0.229
6	887.26	97.738	1.684	945.12	854.47	3.568	0.337
7	1112.93	94.447	5.22	1197.79	991.41	3.329	3.046
8	1240.23	98.206	1.457	1309.67	1197.79	0.551	0.4
9	1375.25	98.687	0.8	1392.61	1357.89	0.138	0.06
10	1436.97	98.265	1.008	1454.33	1415.75	0.196	0.078
11	1465.9	98.31	0.957	1469.76	1454.33	0.099	0.017
12	1570.06	88.169	0.742	1573.91	1504.48	1.986	0.107
13	1656.85	98.149	1.698	1672.28	1645.28	0.129	0.11
14	1718.58	96.732	2.217	1739.79	1691.57	0.475	0.256
15	1751.36	98.538	0.568	1786.8	1739.79	0.134	0.033
16	1805.37	98.333	0.891	1822.73	1789.94	0.177	0.065
17	1847.81	98.166	0.764	1863.24	1822.73	0.247	0.062
18	1923.03	98.315	0.442	1940.39	1913.39	0.171	0.027
19	2187.28	98.227	0.152	2206.57	2156.42	0.373	0.018
20	2370.51	94.673	5.126	2420.66	2353.16	0.579	0.544
21	2600.04	99.581	0.109	2619.33	2576.9	0.057	0.01
22	2661.77	99.449	0.087	2671.41	2642.48	0.051	0.006
23	2760.14	99.553	0.098	2794.85	2744.71	0.083	0.011
24	2818	99.572	0.144	2835.36	2794.85	0.053	0.013
25	2924.09	99.539	0.316	2945.3	2904.8	0.053	0.027
26	3032.1	99.849	0.177	3049.46	3016.67	0.038	0.012
27	3134.33	100.133	0.038	3138.18	3111.18	-0.026	0.005
28	3410.15	89.178	0.278	3415.93	3143.97	7.34	0.741

Comment;
KATK/MnO2

Date/Time; 11/8/2021 3:54:43 PM
No. of Scans;
Resolution;
Apodization;

Lampiran 17. DATA UV-Vis

1. Data Pengaruh Massa KATK Terhadap Pembentukan Nanopartikel MnO_2

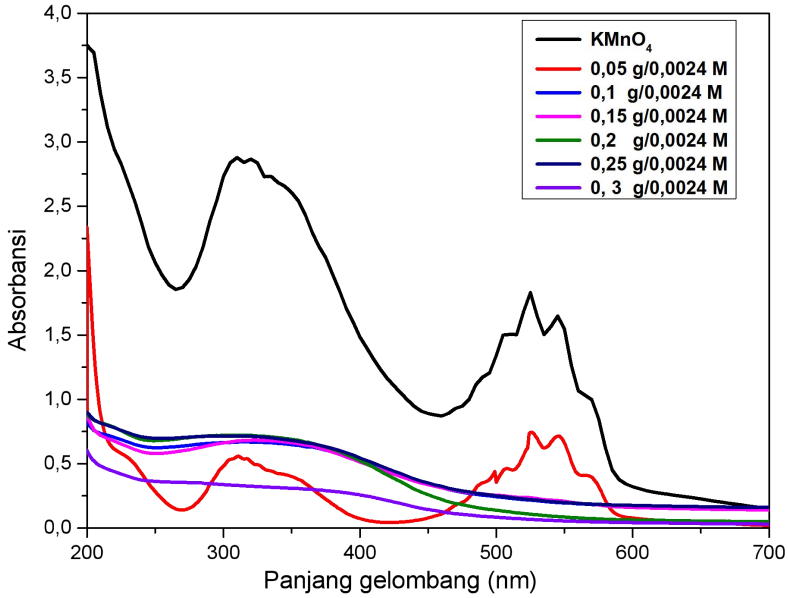

Massa karbon	Absorbansi	Panjang gelombang (nm)	Koloid MnO_2 (%)
0,05	0,826; 0,875; 0,719; 1,094 dan 1,104	545, 525, 508, 317 dan 311	0
0,1	0,67	320	2,91
0,15	0,683	325	2,95
0,2	**0,722**	**313**	**3,13**
0,25	0,716	310	3,11
0,3	-	-	-

2. Data Pengaruh Konsentrasi$KMnO_4$ Terhadap Pembentukan Nanopartikel MnO_2

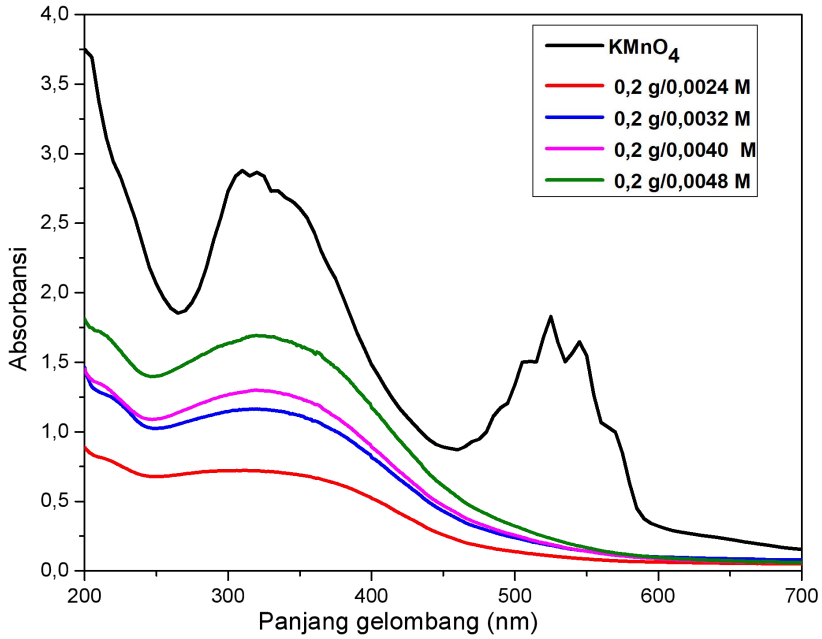

Konsentrasi	Absorbansi	Panjang gelombang (nm)	Koloid MnO_2 (%)
0,0024	0,722	313	3,13
0,0032	1,164	315	3,79
0,004	**1,666**	**326**	**4**
0,0048	1,22	320	2,65

3. Data Pengaruh pH Terhadap Pembentukan Nanopartikel MnO_2

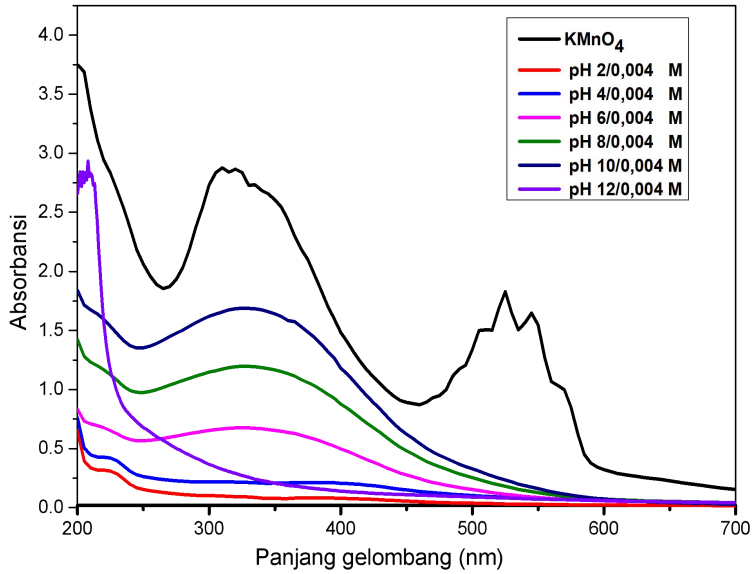

pH	Absorbansi	Panjang gelombang (nm)	Koloid MnO_2 (%)
2	0	0	0
4	0,142	365	0,37
6	0,675	325	1,75
8	1,197	325	3,12
10	**1,688**	**325**	**4,40**
12	2,933 dan 2,844	208 dan 202	0

4. Data Pengaruh Suhu Terhadap Pembentuakan Nanopartikel MnO_2

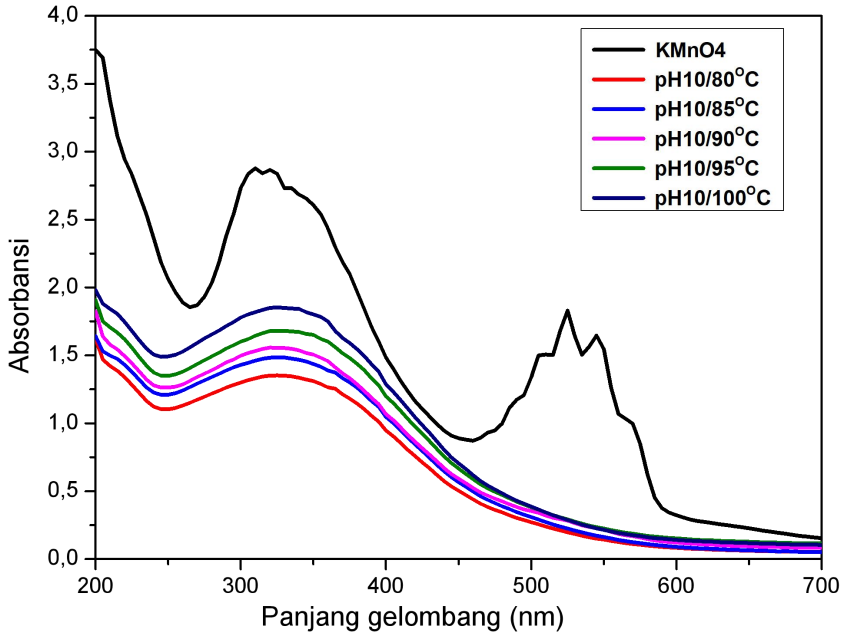

Suhu	Absorbansi	Panjang gelombang (nm)	Koloid MnO_2 (%)
80	1,352	325	3,52
85	1,485	325	3,86
90	1,534	325	4
95	1,688	325	4,4
100	**1,853**	**322**	**4,83**

Lampiran 18. Hasil Karakterisasi SEM EDS

1. Hasil uji SEM KTK

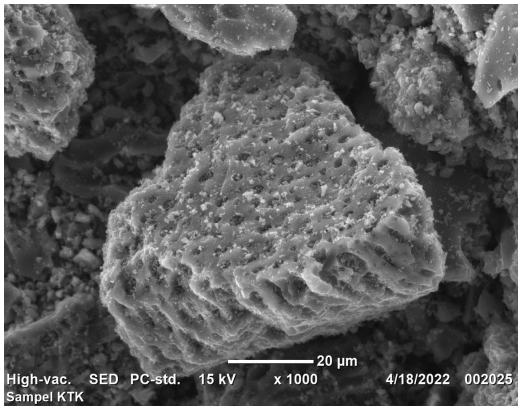

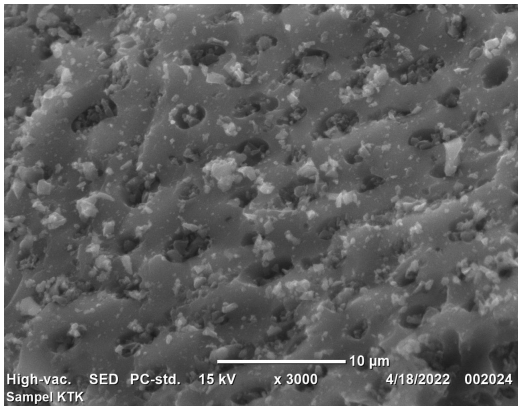

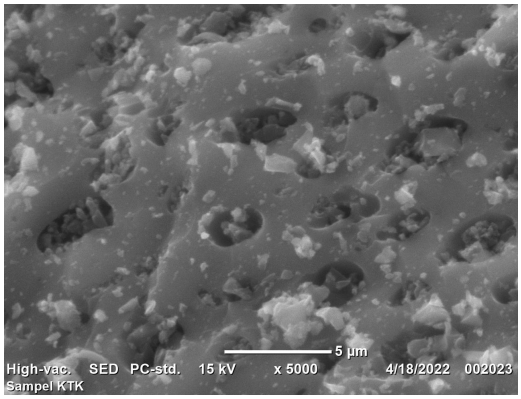

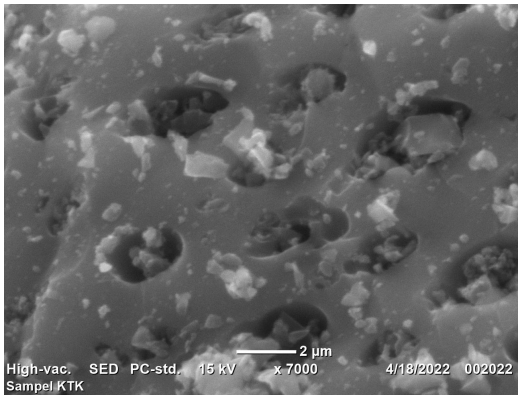

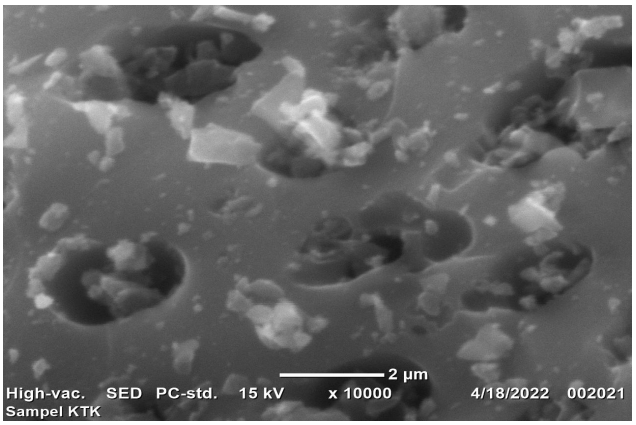

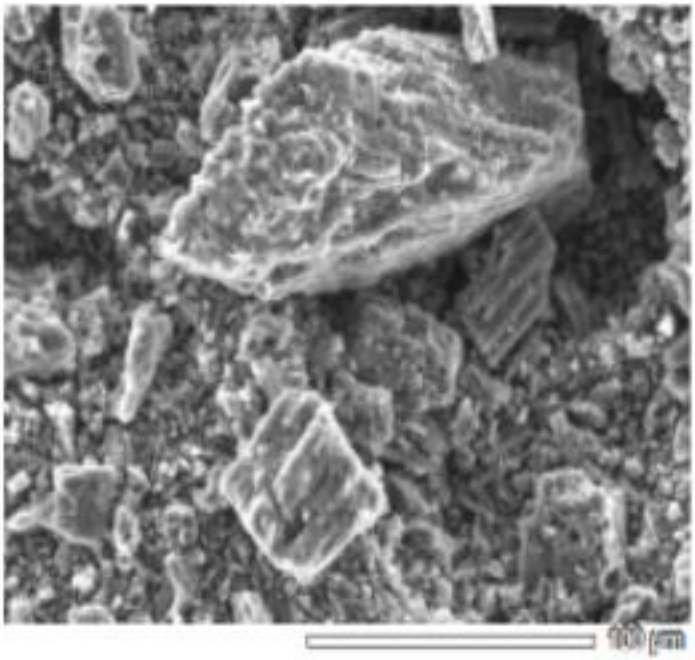

Title	: SM01
Instrument	: JCM-6010PLUS
Volt	: 15.00 kV
Mag.	: x 500
Date	: 2022/04/18
Pixel	: 512 x 384

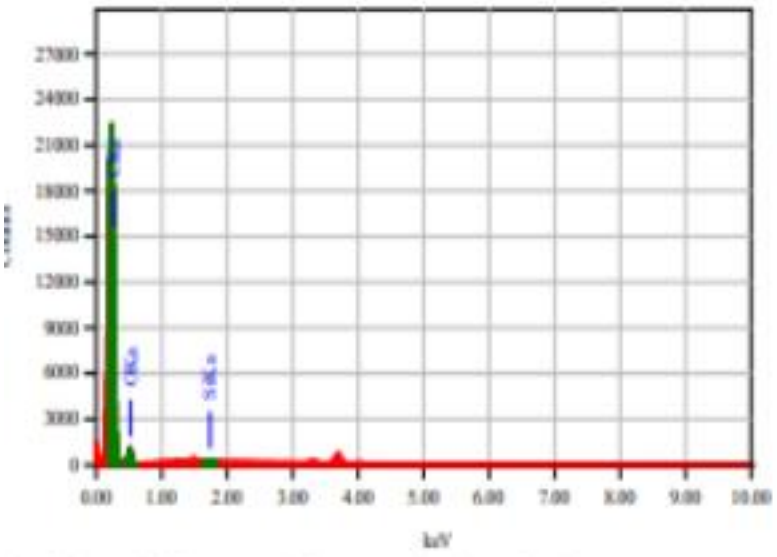

Acquisition Parameter	
Instrument	: JCM-6010PLUS
Acc. Voltage	: 15.0 kV
Probe Current	: 1.00000 nA
PHA mode	: T3
Real Time	: 51.76 sec
Live Time	: 50.00 sec
Dead Time	: 3 %
Counting Rate	: 8407 cps
Energy Range	: 0 - 20 keV

hin Film Standardless Standardless Quantitative Analysis
itting Coefficient : 0.9557

Element	(keV)	Mass%	Counts	Sigma	Atom%	Compound	Mass%	Cation	K
C K (Ref.)	0.277	93.51	31413.23	0.33	95.15				1.0000
O K	0.525	6.17	5358.24	0.10	4.71				0.3869
I K	1.739	0.32	340.19	0.04	0.14				0.3164
otal		100.00			100.00				

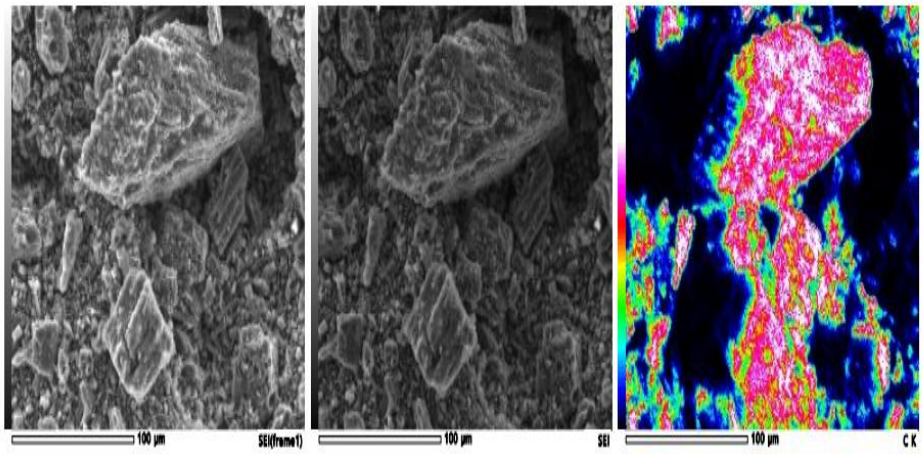
100 µm
SEI(frame1)
100 µm
SEI
100 µm
C K

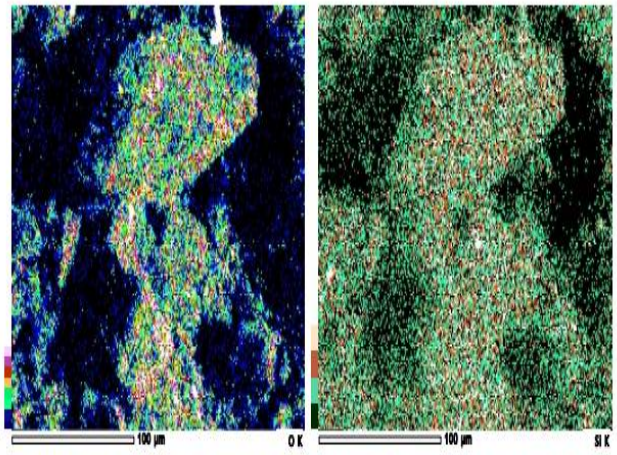
100 µm
O K
100 µm
Si K

2. Hasil uji SEM KATK

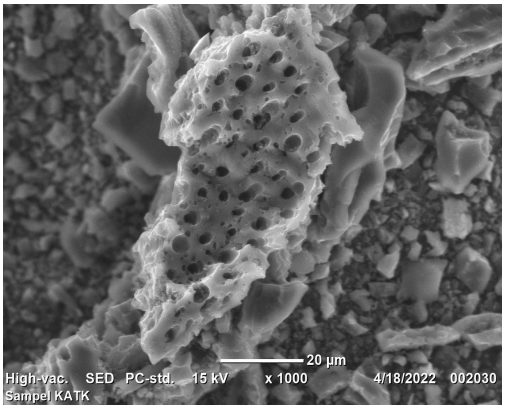

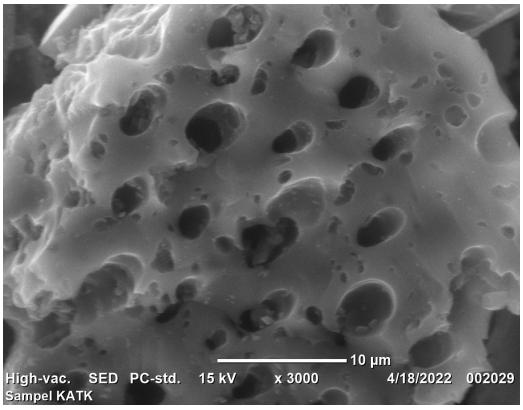

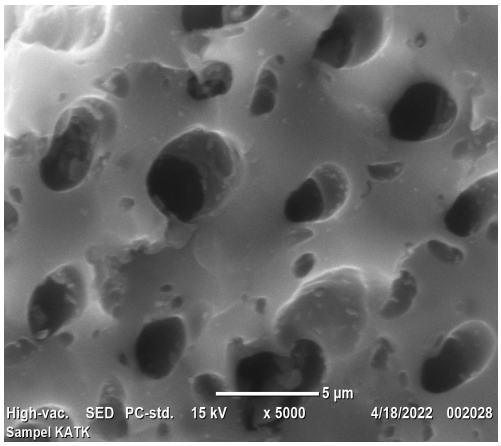

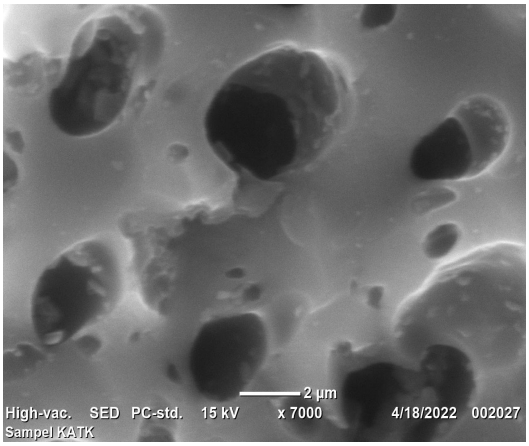

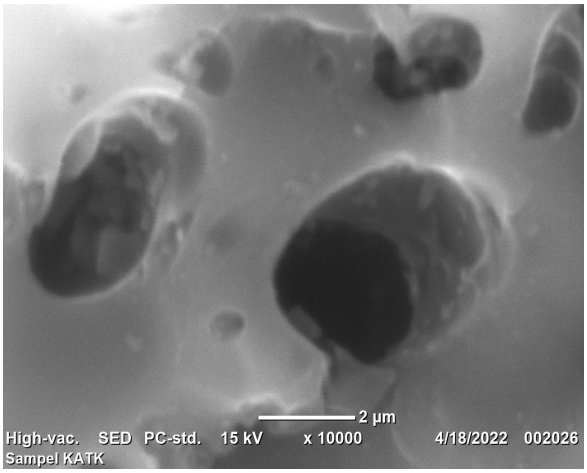

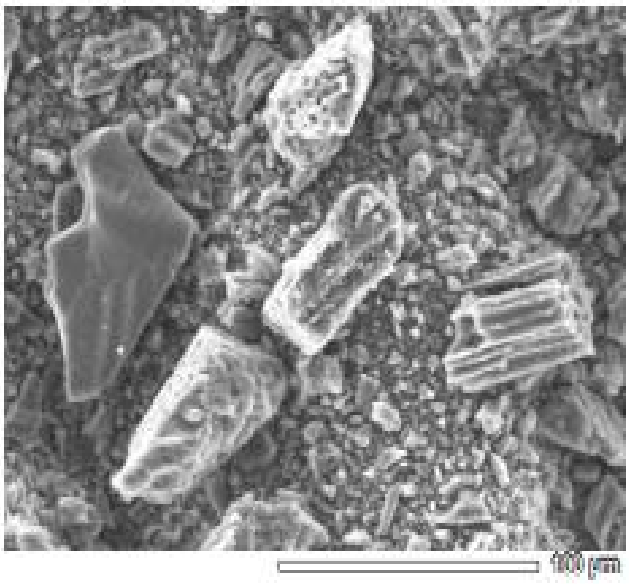

Title	: EMAS
Instrument	: JCM-6000PLUS
Volt	: 15.00 kV
Mag.	: x 500
Date	: 2022/04/15
Pixel	: 512 x 384

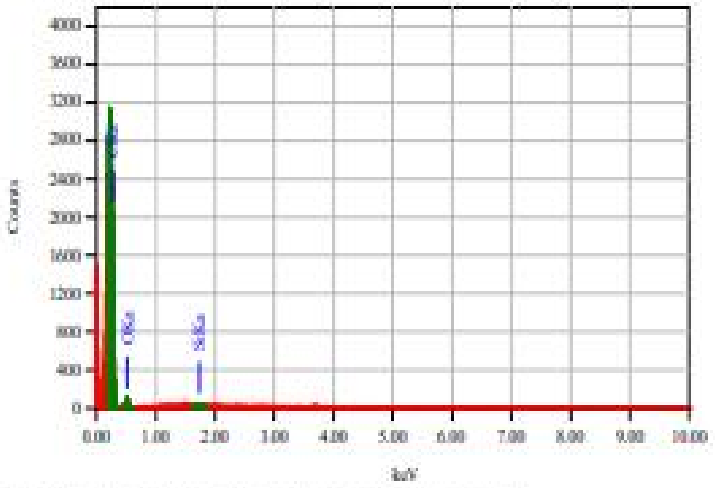

Acquisition Parameter
Instrument : JCM-6000PLUS
Acc. Voltage : 15.0 kV
Probe Current: 1.00000 nA
PHA mode : T3
Real Time : 50.89 sec
Live Time : 50.00 sec
Dead Time : 1 %
Counting Rate: 1253 cps
Energy Range : 0 - 20 keV

Thin Film Standardless Standardless quantitative analysis
Fitting Coefficient : 0.8954

Element	(keV)	Mass%	Counts	Sigma	Atom%	Compound	Mass% ration	K
C K (Ref.)	0.277	95.32	6208.27	0.52	96.60			1.0000
O K	0.525	4.18	477.14	0.22	3.18			0.3869
Si K	1.739	0.49	69.29	0.17	0.21			0.3144
Total		100.00			100.00			

View002

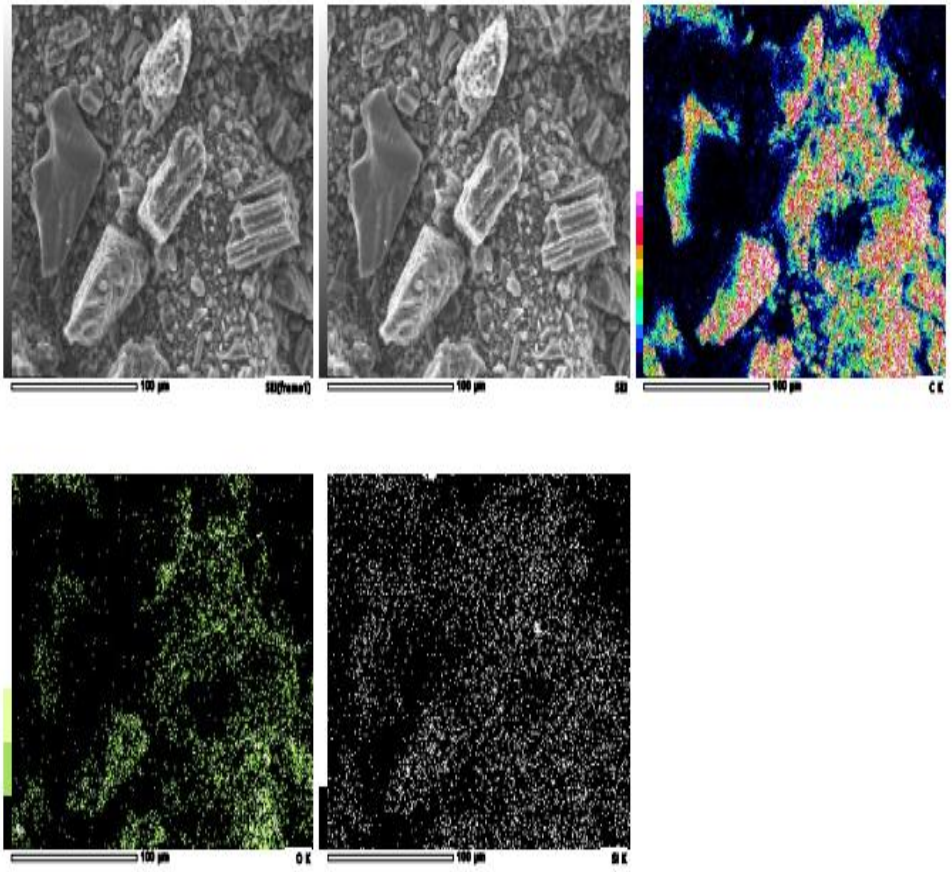

JEOL

3.Hasil uji SEM KATK+MnO_2

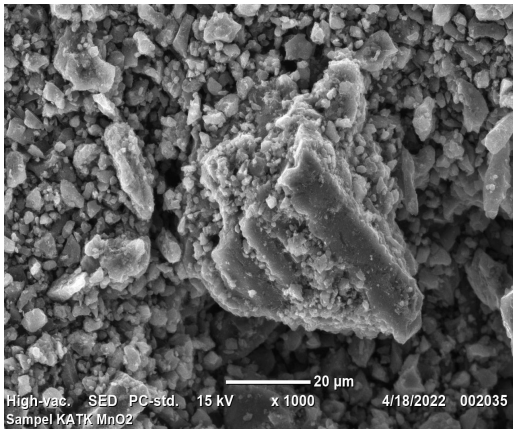

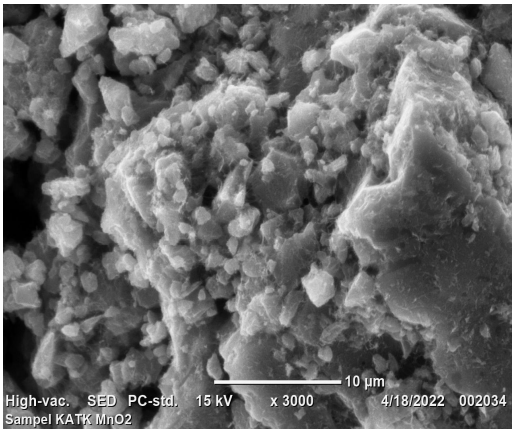

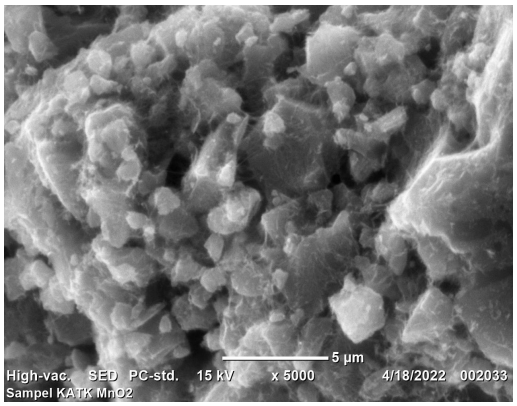

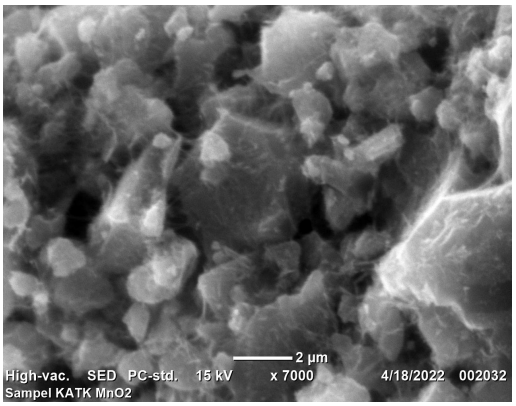

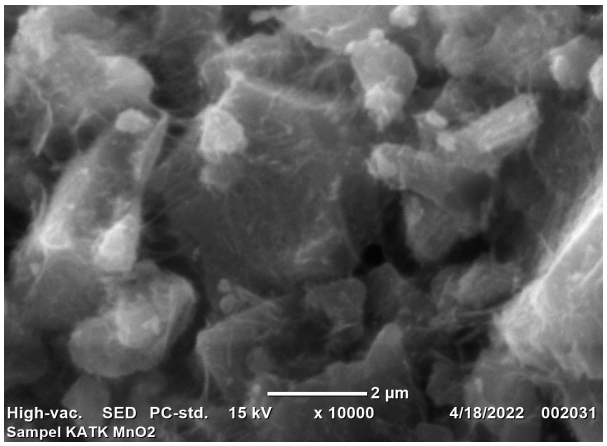

View003

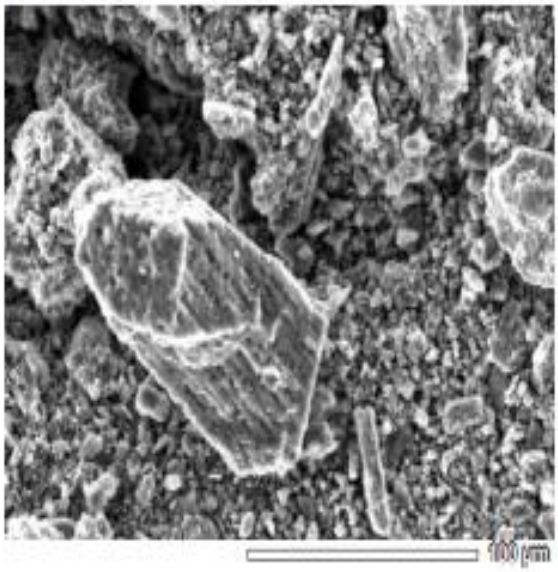

Title	: DM01
Instrument	: JCM-6000PLUS
Volt	: 15.00 kV
Mag.	: x 500
Date	: 2022/04/19
Pixel	: 512 x 384

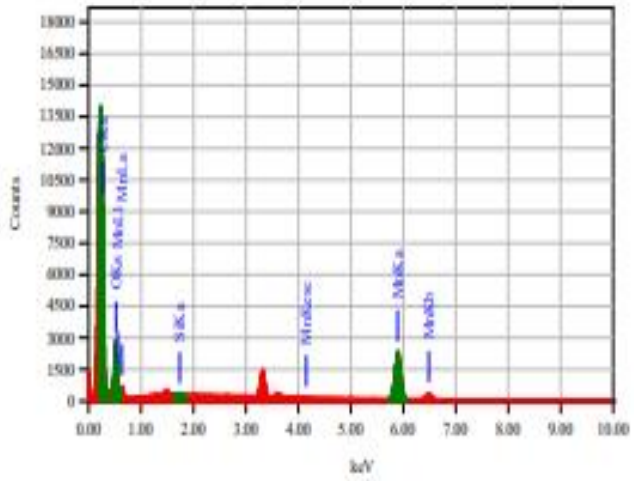

Acquisition Parameter
Instrument : JCM-6000PLUS
Acc. Voltage : 15.0 kV
Probe Current: 1.00000 nA
PHA mode : T3
Real Time : 51.81 sec
Live Time : 50.00 sec
Dead Time : 3 %
Counting Rate: 8308 cps
Energy Range : 0 - 20 keV

Thin Film Standardless Standardless Quantitative Analysis
Fitting Coefficient : 0.5622

Element	(keV)	Mass%	Counts	Sigma	Atom%	Compound	Mass%	Cation	K
C K	0.277	33.08	17938.69	0.16	62.87				0.9475
O K	0.525	9.16	12835.46	0.09	13.07				0.3666
Si K	1.739	0.17	298.73	0.04	0.14				0.2879
Mn K* (Ref.)	5.894	57.58	29576.91	0.48	23.92				1.0000
Total		100.00			100.00				

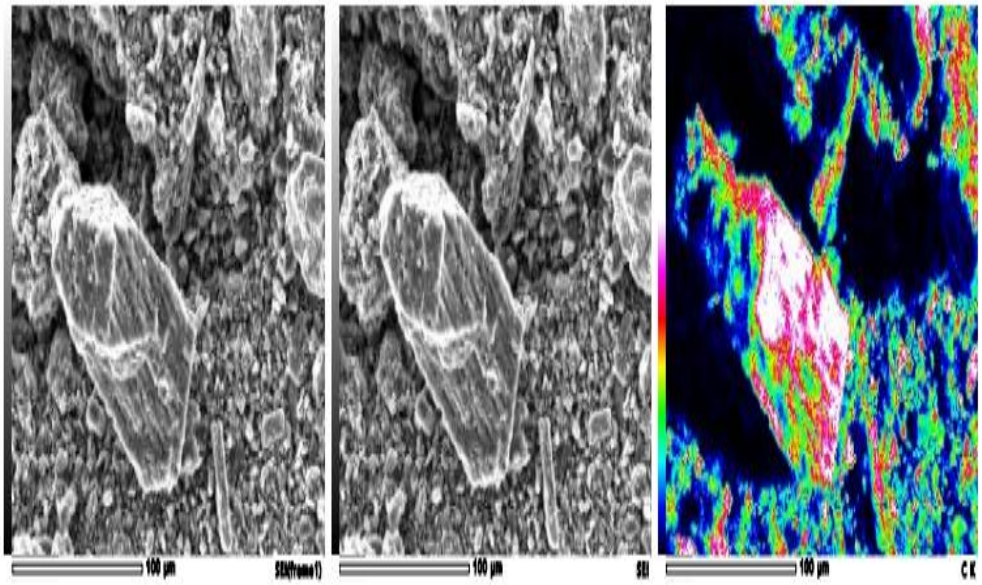

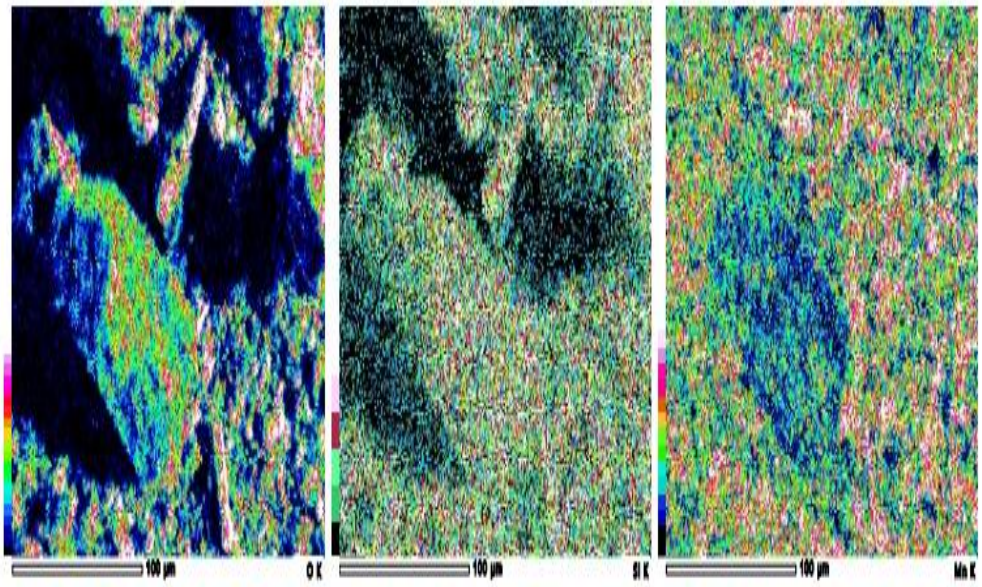

Lampiran 19. Hasil Karakterisasi SAA

1. KTK

micromeritics

TriStar II 3020 2.00 TriStar II 3020 Version 2.00 Unit 1 Port 1 Serial #: 1108 Page: 1

Sample: KTK
Operator: Sarah
Submitter: 37897
File: C:\TriStar II 3020\data\SAMPEL\2022\Mei\Sample ID...\KTK.SMP

Started: 5/10/2022 6:39:56 AM
Completed: 5/10/2022 12:03:41 PM
Report Time: 5/12/2022 1:00:40 PM
Sample Mass: 0.6066 g
Cold Free Space: 32.1203 cm³
Low Pressure Dose: None
Automatic Degas: No

Analysis Adsorptive: N2
Analysis Bath Temp.: -195.850 °C
Thermal Correction: No
Warm Free Space: 10.8393 cm³ Measured
Equilibration Interval: 5 s
Sample Density: 1.000 g/cm³

Summary Report

Surface Area

Single point surface area at P/Po = 0.312478818:	351.3653 m²/g
BET Surface Area:	351.0143 m²/g
t-Plot Micropore Area:	266.7521 m²/g
t-Plot External Surface Area:	84.2622 m²/g
BJH Adsorption cumulative surface area of pores between 1.7000 nm and 300.0000 nm diameter:	77.700 m²/g
BJH Desorption cumulative surface area of pores between 1.7000 nm and 300.0000 nm diameter:	76.3209 m²/g
D-H Adsorption cumulative surface area of pores between 1.7000 nm and 300.0000 nm diameter:	82.281 m²/g
D-H Desorption cumulative surface area of pores between 1.7000 nm and 300.0000 nm diameter:	69.0026 m²/g

Pore Volume

Single point adsorption total pore volume of pores less than 317.8681 nm diameter at P/Po = 0.993943706:	0.221368 cm³/g
t-Plot micropore volume:	0.138871 cm³/g
BJH Adsorption cumulative volume of pores between 1.7000 nm and 300.0000 nm diameter:	0.075780 cm³/g
BJH Desorption cumulative volume of pores between 1.7000 nm and 300.0000 nm diameter:	0.073420 cm³/g

Pore Size

Adsorption average pore width (4V/A by BET):	2.52262 nm
BJH Adsorption average pore diameter (4V/A):	3.9001 nm
BJH Desorption average pore diameter (4V/A):	3.8480 nm
D-H Adsorption average pore diameter (4V/A):	4.4201 nm
D-H Desorption average pore diameter (4V/A):	4.0071 nm

micromeritics

Sample: KTK
Operator: Sarah
Submitter: 37897
File: C:\TriStar II 3020\data\SAMPEL\2022\Mei\Sample ID...\KTK.SMP

Started: 5/10/2022 6:39:56 AM
Completed: 5/10/2022 12:03:41 PM
Report Time: 5/12/2022 1:00:40 PM
Sample Mass: 0.6066 g
Cold Free Space: 32.1203 cm³
Low Pressure Dose: None
Automatic Degas: No

Analysis Adsorptive: N2
Analysis Bath Temp.: -195.850 °C
Thermal Correction: No
Warm Free Space: 10.8393 cm³ Measured
Equilibration Interval: 5 s
Sample Density: 1.000 g/cm³

Freundlich

Qm C: 88.1658 ± 0.3140 cm³/g STP

m: 19.3292 ± 0.6727

Temkin

q·alpha/Qm: 0.115434 ± 0.005706 kJ/mol·(cm³/g STP)

A: 5540294.1207 ± 4431874.8891 mmHg

DFT Pore Size

Volume in Pores	<	1.483 nm	:	0.13452 cm³/g
Total Volume in Pores	<=	216.632 nm	:	0.18737 cm³/g
Area in Pores	>	216.632 nm	:	1.630 m²/g
Total Area in Pores	>=	1.483 nm	:	26.511 m²/g

DFT Surface Energy

Total Area : 533.318 m²/g

Nanoparticle Size:

Average Particle Size 17.0933 nm

Horvath-Kawazoe

Maximum pore volume at P/Po = 0.993943706: 0.221368 cm³/g

Median pore width: 1.0512 nm

MP-Method

Cumulative surface area of pores between 0.28688 nm and 1.96000 nm hydraulic radius: 559.4454 m²/g

Cumulative pore volume of pores between 0.28688 nm and 1.96000 nm hydraulic radius: 0.198571 cm³/g

Average pore hydraulic radius (V/A): 0.35494 nm

micromeritics

TriStar II 3020 2.00 TriStar II 3020 Version 2.00 Unit 1 Port 1 Serial #: 1108 Page 4

Sample: KTK
Operator: Sarah
Submitter: 37897
File: C:\TriStar II 3020\data\SAMPEL\2022\Mei\Sample ID...\KTK.SMP

Started: 5/10/2022 6:39:58 AM
Completed: 5/10/2022 12:03:41 PM
Report Time: 5/12/2022 1:00:40 PM
Sample Mass: 0.6066 g
Cold Free Space: 32.1203 cm³
Low Pressure Dose: None
Automatic Degas: No

Analysis Adsorptive: N2
Analysis Bath Temp.: -195.850 °C
Thermal Correction: No
Warm Free Space: 10.8393 cm³ Measured
Equilibration Interval: 5 s
Sample Density: 1.000 g/cm³

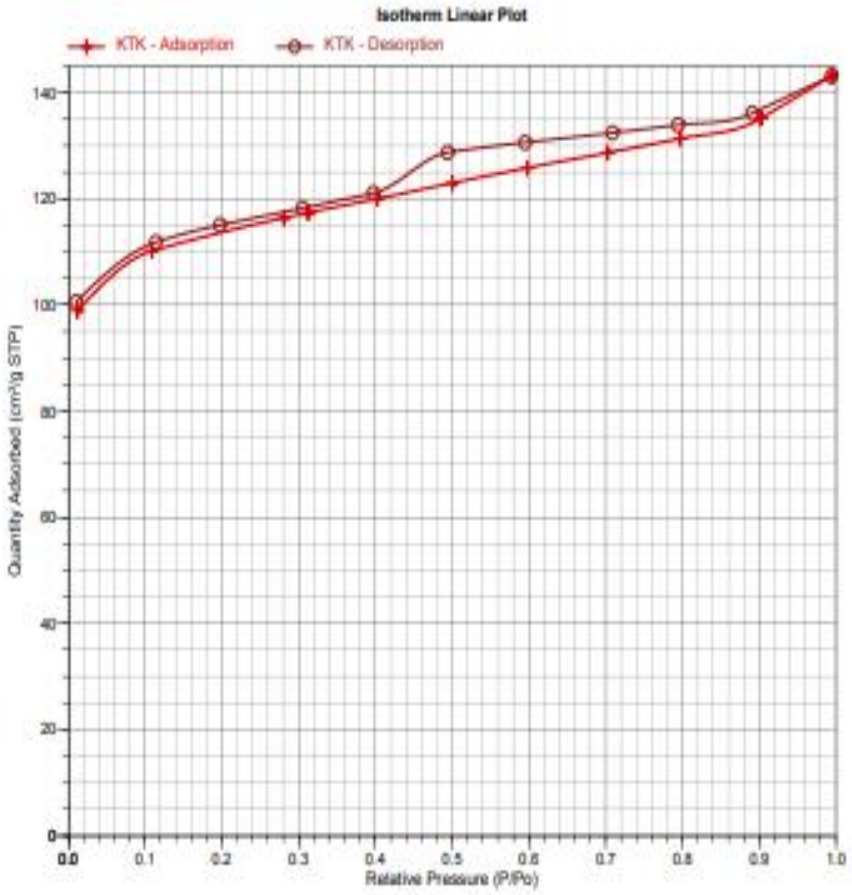

2. KATK

micromeritics

TriStar II 3020 2.00 TriStar II 3020 Version 2.00 Unit 1 Port 2 Serial #: 1108 Page 1

Sample: KATK
Operator: Sarah
Submitter: 37897
File: C:\TriStar II 3020\data\SAMPEL\2022\Mei\Sample I...\KATK.SMP

Started: 5/10/2022 6:39:56 AM
Completed: 5/10/2022 12:03:41 PM
Report Time: 5/12/2022 1:01:23 PM
Sample Mass: 0.5833 g
Cold Free Space: 33.6423 cm³
Low Pressure Dose: None
Automatic Degas: No

Analysis Adsorptive: N2
Analysis Bath Temp.: -195.850 °C
Thermal Correction: No
Warm Free Space: 11.1636 cm³ Measured
Equilibration Interval: 5 s
Sample Density: 1.000 g/cm³

Summary Report

Surface Area

Single point surface area at P/Po = 0.315935998:	517.7737 m²/g
BET Surface Area:	518.5501 m²/g
t-Plot Micropore Area:	361.8623 m²/g
t-Plot External Surface Area:	156.6878 m²/g
BJH Adsorption cumulative surface area of pores between 1.7000 nm and 300.0000 nm diameter:	145.580 m²/g
BJH Desorption cumulative surface area of pores between 1.7000 nm and 300.0000 nm diameter:	143.0602 m²/g
D-H Adsorption cumulative surface area of pores between 1.7000 nm and 300.0000 nm diameter:	115.687 m²/g
D-H Desorption cumulative surface area of pores between 1.7000 nm and 300.0000 nm diameter:	128.0632 m²/g

Pore Volume

Single point adsorption total pore volume of pores less than 275.6684 nm diameter at P/Po = 0.993011555:	0.329341 cm³/g
t-Plot micropore volume:	0.189350 cm³/g
BJH Adsorption cumulative volume of pores between 1.7000 nm and 300.0000 nm diameter:	0.127683 cm³/g
BJH Desorption cumulative volume of pores between 1.7000 nm and 300.0000 nm diameter:	0.125727 cm³/g

Pore Size

Adsorption average pore width (4V/A by BET):	2.54047 nm
BJH Adsorption average pore diameter (4V/A):	3.5082 nm
BJH Desorption average pore diameter (4V/A):	3.5154 nm
D-H Adsorption average pore diameter (4V/A):	3.9867 nm
D-H Desorption average pore diameter (4V/A):	3.6865 nm

micromeritics

Sample: KATK
Operator: Sarah
Submitter: 37897
File: C:\TriStar II 3020\data\SAMPEL\2022\Mei\Sample I...\KATK.SMP

Started: 5/10/2022 6:39:56 AM
Completed: 5/10/2022 12:03:41 PM
Report Time: 5/12/2022 1:01:24 PM
Sample Mass: 0.5833 g
Cold Free Space: 33.6423 cm³
Low Pressure Dose: None
Automatic Degas: No

Analysis Adsorptive: N2
Analysis Bath Temp.: -195.850 °C
Thermal Correction: No
Warm Free Space: 11.1636 cm³ Measured
Equilibration Interval: 5 s
Sample Density: 1.000 g/cm³

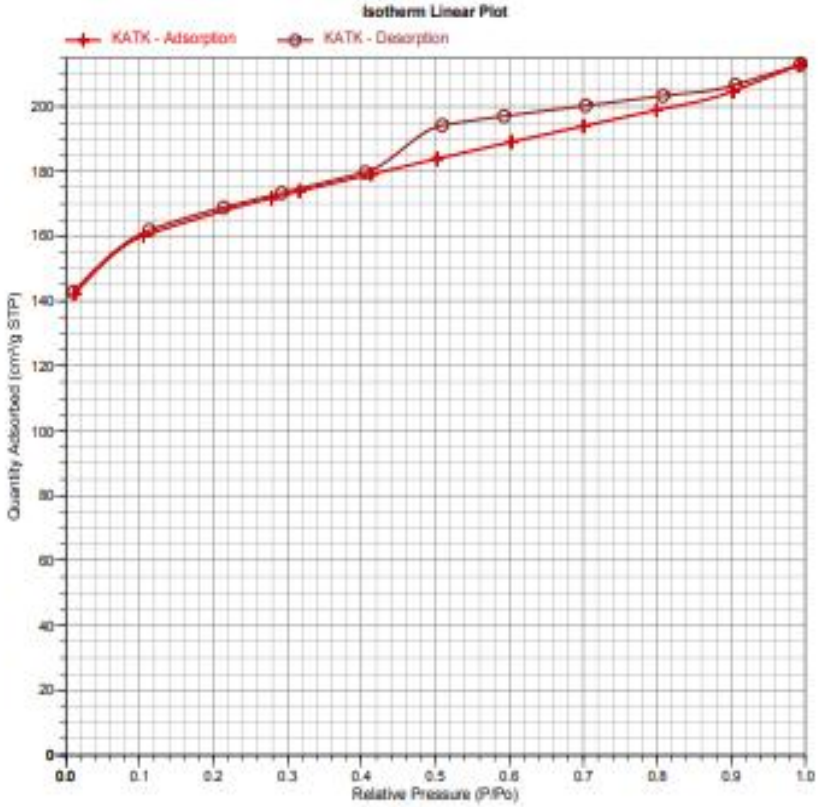

3.KATK+MnO_2

micromeritics

TriStar II 3020 2.00 TriStar II 3020 Version 2.00 Unit 1 Port 3 Serial #: 1108 Page 1

Sample: KATK-MnO2
Operator: Sarah
Submitter: 37897
File: C:\TriStar II 3020\data\SAMPEL\2022\Mei\Sam...\KATK-MnO2.SMP

Started: 5/10/2022 6:39:56 AM
Completed: 5/10/2022 12:03:42 PM
Report Time: 5/12/2022 1:03:15 PM
Sample Mass: 0.3707 g
Cold Free Space: 32.9975 cm³
Low Pressure Dose: None
Automatic Degas: No

Analysis Adsorptive: N2
Analysis Bath Temp.: -195.850 °C
Thermal Correction: No
Warm Free Space: 11.2842 cm³ Measured
Equilibration Interval: 5 s
Sample Density: 1.000 g/cm³

Summary Report

Surface Area

Single point surface area at P/Po = 0.324924007:	392.3282 m²/g
BET Surface Area:	395.6897 m²/g
t-Plot Micropore Area:	259.2675 m²/g
t-Plot External Surface Area:	136.4222 m²/g
BJH Adsorption cumulative surface area of pores between 1.7000 nm and 300.0000 nm diameter:	118.474 m²/g
BJH Desorption cumulative surface area of pores between 1.7000 nm and 300.0000 nm diameter:	125.9909 m²/g
D-H Adsorption cumulative surface area of pores between 1.7000 nm and 300.0000 nm diameter:	102.193 m²/g
D-H Desorption cumulative surface area of pores between 1.7000 nm and 300.0000 nm diameter:	113.7304 m²/g

Pore Volume

Single point adsorption total pore volume of pores less than 257.2334 nm diameter at P/Po = 0.992506284:	0.290335 cm³/g
t-Plot micropore volume:	0.136829 cm³/g
BJH Adsorption cumulative volume of pores between 1.7000 nm and 300.0000 nm diameter:	0.140700 cm³/g
BJH Desorption cumulative volume of pores between 1.7000 nm and 300.0000 nm diameter:	0.141620 cm³/g

Pore Size

Adsorption average pore width (4V/A by BET):	2.93498 nm
BJH Adsorption average pore diameter (4V/A):	4.7504 nm
BJH Desorption average pore diameter (4V/A):	4.4962 nm
D-H Adsorption average pore diameter (4V/A):	5.1629 nm
D-H Desorption average pore diameter (4V/A):	4.7112 nm

micromeritics

Sample: KTK
Operator: Sarah
Submitter: 37897
File: C:\TriStar II 3020\data\SAMPEL\2022\Mei\Sample ID...\KTK.SMP

Started:	5/10/2022 6:39:56 AM	Analysis Adsorptive:	N2
Completed:	5/10/2022 12:03:41 PM	Analysis Bath Temp.:	-195.850 °C
Report Time:	5/12/2022 1:00:40 PM	Thermal Correction:	No
Sample Mass:	0.6066 g	Warm Free Space:	10.8393 cm³ Measured
Cold Free Space:	32.1203 cm³	Equilibration Interval:	5 s
Low Pressure Dose:	None	Sample Density:	1.000 g/cm³
Automatic Degas:	No		

Freundlich

Qm·C: 88.1658 ± 0.3140 cm³/g STP

m: 19.3292 ± 0.6727

Temkin

q·alpha/Qm: 0.115434 ± 0.005706 kJ/mol (cm³/g STP)

A: 5540294.1207 ± 4431874.8891 mmHg

DFT Pore Size

Volume in Pores	<	1.483 nm	:	0.13452 cm³/g
Total Volume in Pores	<=	216.632 nm	:	0.18737 cm³/g
Area in Pores	>	216.632 nm	:	1.630 m²/g
Total Area in Pores	>=	1.483 nm	:	26.511 m²/g

DFT Surface Energy

Total Area : 533.318 m²/g

Nanoparticle Size:

Average Particle Size 17.0933 nm

Horvath-Kawazoe

Maximum pore volume at P/Po = 0.993943706: 0.221368 cm³/g

Median pore width: 1.0512 nm

MP-Method

Cumulative surface area of pores between 0.26888 nm and 1.96000 nm hydraulic radius: 559.4454 m²/g

Cumulative pore volume of pores between 0.26888 nm and 1.96000 nm hydraulic radius: 0.198571 cm³/g

Average pore hydraulic radius (V/A): 0.35494 nm

micromeritics

Sample: KATK-MnO2
Operator: Sarah
Submitter: 37897
File: C:\TriStar II 3020\data\SAMPEL\2022\Mei\Sam..\KATK-MnO2.SMP

Started:	5/10/2022 6:39:56 AM	Analysis Adsorptive:	N2
Completed:	5/10/2022 12:03:42 PM	Analysis Bath Temp.:	-195.850 °C
Report Time:	5/12/2022 1:03:15 PM	Thermal Correction:	No
Sample Mass:	0.3707 g	Warm Free Space:	11.2842 cm³ Measured
Cold Free Space:	32.9975 cm³	Equilibration Interval:	5 s
Low Pressure Dose:	None	Sample Density:	1.000 g/cm³
Automatic Degas:	No